J|A|C|S
ARTICLES

Published on Web 09/15/2009

# Thermodynamic Studies and Hydride Transfer Reactions from a Rhodium Complex to $BX_3$ Compounds

Michael T. Mock, Robert G. Potter, Donald M. Camaioni, Jun Li,[§]
William G. Dougherty,[†] W. Scott Kassel,[†] Brendan Twamley,[‡] and Daniel L. DuBois*

*Pacific Northwest National Laboratory, P.O. Box 999, Richland, Washington 99352,*
*Department of Chemistry, Villanova University, Villanova, Pennsylvania 19085, and*
*Department of Chemistry, University of Idaho, Moscow, Idaho 83844*

Received June 26, 2009; E-mail: daniel.dubois@pnl.gov

***Abstract:*** This study examines the use of transition-metal hydride complexes that can be generated by the heterolytic cleavage of $H_2$ gas to form B−H bonds. Specifically, these studies are focused on providing a reliable and quantitative method for determining when hydride transfer from transition-metal hydrides to three-coordinate $BX_3$ (X = OR, SPh, F, H; R = Ph, *p*-$C_6H_4OMe$, $C_6F_5$, $^tBu$, $Si(Me)_3$) compounds will be favorable. This involves both experimental and theoretical determinations of hydride transfer abilities. Thermodynamic hydride donor abilities ($\Delta G^\circ_{H^-}$) were determined for $HRh(dmpe)_2$ and $HRh(depe)_2$, where dmpe = 1,2-bis(dimethylphosphinoethane) and depe = 1,2-bis(diethylphosphinoethane), on a previously established scale in acetonitrile. This hydride donor ability was used to determine the hydride donor ability of $[HBEt_3]^-$ on this scale. Isodesmic reactions between $[HBEt_3]^-$ and selected $BX_3$ compounds to form $BEt_3$ and $[HBX_3]^-$ were examined computationally to determine their relative hydride affinities. The use of these scales of hydride donor abilities and hydride affinities for transition-metal hydrides and $BX_3$ compounds is illustrated with a few selected reactions relevant to the regeneration of ammonia borane. Our findings indicate that it is possible to form B−H bonds from B−X bonds, and the extent to which $BX_3$ compounds are reduced by transition-metal hydride complexes forming species containing multiple B−H bonds depends on the heterolytic B−X bond energy. An example is the reduction of $B(SPh)_3$ using $HRh(dmpe)_2$ in the presence of triethylamine to form $Et_3N{-}BH_3$ in high yields.

## Introduction

As the need for clean and renewable sources of energy grows, attention has increasingly focused on using hydrogen as an alternative to hydrocarbon fuels.[1] The development of new hydrogen storage methods and materials has become an area of intense research, and safe and convenient methods to transport, store, and distribute hydrogen continue to evolve. In particular, ammonia borane (AB, $NH_3BH_3$) with a gravimetric density of 19.6 wt % $H_2$ is a promising candidate for hydrogen storage.[2] Several important studies addressing various methods of hydrogen release from AB have been published,[3] however, only a few reports on the regeneration of AB from dehydrogenated material have appeared in the literature.[4] These methods use energy intensive reagents such as $LiAlH_4$ or $MgH_2$ to achieve B−H bond formation from B−O or B−Cl bonds resulting from spent fuel digestion. As a result, an energy efficient method for the regeneration of AB remains a significant challenge for using AB as a hydrogen storage material.

As an alternative approach to AB regeneration, we are exploring the use of transition-metal hydride complexes that can be generated by the heterolytic cleavage of $H_2$ gas to regenerate B−H bonds from B−X bonds in model compounds potentially generated from the digestion of dehydrogenated material with alcohols,[5] phenols, or thiols[6] to form $BX_3$ compounds ($BX_3$ = aryl, alkyl or thio borate esters). In previous publications, we have focused on understanding the structural and electronic features controlling the hydride

---

[†] Villanova University.

[‡] University of Idaho.

[§] Present address: Department of Chemistry, Tsinghua University, Beijing, China.

(1) Lubitz, W.; Tumas, W. *Chem. Rev.* **2007**, *107*, 3900.

(2) (a) Marder, T. B. *Angew. Chem., Int. Ed.* **2007**, *46*, 8116. (b) Stephens, F. H.; Pons, V.; Baker, T. R. *J. Chem. Soc., Dalton. Trans.* **2007**, *25*, 2613.

(3) (a) Baitalow, F.; Baumann, J.; Wolf, G.; Jaenicke-Rossler, K.; Leitner, G. *Thermochim. Acta* **2002**, *391*, 159. (b) Baumann, J.; Baitalow, E.; Wolf, G. *Thermochim. Acta* **2005**, *430*, 9. (c) Keaton, R. J.; Blacquiere, J. M.; Baker, R. T. *J. Am. Chem. Soc.* **2007**, *129*, 1844. (d) Stephens, F. H.; Baker, R. T.; Matus, M. H.; Grant, D. J.; Dixon, D. A. *Angew. Chem., Int. Ed.* **2007**, *46*, 746. (e) Denney, M. C.; Pons, V.; Hebden, T. J.; Heinekey, D. M.; Goldberg, K. I. *J. Am. Chem. Soc.* **2006**, *128*, 12048. (f) Bluhm, M. E.; Bradley, M. G.; Butterick, R.; Kusari, U.; Sneddon, L. G. *J. Am. Chem. Soc.* **2006**, *128*, 7748. (g) Gutowska, A.; Li, L. Y.; Shin, Y. S.; Wang, C. M. M.; Li, X. H. S.; Linehan, J. C.; Smith, R. S.; Kay, B. D.; Schmid, B.; Shaw, W.; Gutowski, M.; Autrey, T. *Angew. Chem., Int. Ed.* **2005**, *44*, 3578.

(4) (a) Ramachandran, P. V.; Gagare, P. D. *Inorg. Chem.* **2007**, *46*, 7810. (b) Hausdorf, S.; Baitalow, F.; Wolf, G.; Mertens, F. O. R. L. *Int. J. Hydrogen Energy* **2008**, *33*, 608.

(5) Camaioni, D. M.; Heldebrant, D. J.; Linehan, J. C.; Shaw, W. J.; Li, J.; DuBois, D. L.; Autrey, T. *Prepr. Pap.—Am. Chem. Soc., Div. Fuel Chem.* **2007**, *52*, 509.

(6) (a) Davis, B. L.; Dixon, D. A.; Garner, E. B.; Gordon, J. C.; Matus, M. H.; Scott, B.; Stephens, F. H. *Angew. Chem., Int. Ed.* **2009**, *48*, 6812. (b) Hamilton, C. W.; Baker, R. T.; Staubitz, A.; Manners, I. *Chem. Soc. Rev.* **2009**, *38*, 279.

**10.1021/ja905287q CCC: $40.75**

donor abilities of transition-metal hydride complexes with chelating diphosphine ligands, e.g. HM(diphosphine)$_2$ and [HM′(diphosphine)$_2$]$^+$ complexes where M is Co or Rh and M′ is Ni, Pd, or Pt.[7] These complexes exhibit a large range of hydride donor abilities with the free energies associated with reaction 1 ($\Delta G°_{H^-}$) ranging from 34 to 76 kcal/mol,[8] with smaller values of $\Delta G°_{H^-}$ representing better hydride donors.

$$[\mathrm{HM(diphosphine)_2}]^{n+} \rightarrow [\mathrm{M(diphosphine)_2}]^{(n+1)+} + \mathrm{H}^- \qquad (1)$$

These studies revealed that strong hydride donors are favored by electron-donating substituents on the diphosphine ligands[9] and ligands with small natural bite angles.[10] In addition, second row transition-metal hydride complexes are better hydride donors than either the first or third row complexes.[11] This led us to study HRh(dmpe)$_2$, where dmpe = 1,2-bis(dimethylphosphinoethane), one of the strongest hydride donors of this type, for its ability to transfer a hydride ligand to triethylborane, BEt$_3$, to form [HBEt$_3$]$^-$, Super-Hydride.[12] This is important because HRh(dmpe)$_2$ can be generated from H$_2$ and [Rh(dmpe)$_2$]$^+$ in the presence of a strong base, potentially providing a more direct route for the production of boron hydride compounds from hydrogen.

Herein we describe our efforts to provide a reliable and quantitative method for determining when hydride transfer from transition-metal hydrides to three-coordinate BX$_3$ compounds will be favorable. This involves both experimental and theoretical determinations of hydride transfer abilities. In addition to understanding the thermodynamic feasibility of transferring a hydride ligand from a transition-metal hydride to boron compounds, it is also important that the resulting [HBX$_3$]$^-$ anions undergo ligand redistribution reactions or further reaction with the transition-metal hydride to form species containing multiple B−H bonds. To achieve this goal, hydride transfer reactions from HRh(dmpe)$_2$ to B(SPh)$_3$ were studied and shown to result in the cleavage of B−S bonds and the formation of multiple B−H bonds.

## Results and Discussion

The main objective of this research is to provide a reliable and quantitative method for predicting when B−H bond formation from transition-metal hydrides will be favorable. This can be achieved in three steps. First, the hydride donor ability ($\Delta G°_{H^-}$) of HRh(dmpe)$_2$ on the previously established scale in acetonitrile is determined. Second, this hydride donor ability is used to determine the hydride donor ability of [HBEt$_3$]$^-$ on this scale. Third, a series of isodesmic reactions between [HBEt$_3$]$^-$ and BX$_3$ compounds to form BEt$_3$ and [HBX$_3$]$^-$ are studied computationally to determine the relative hydride affinities of the BX$_3$ compounds. The result is a series of transition-metal hydride complexes of known hydride donor abilities obtained from previous studies and a series of BX$_3$ compounds with hydride acceptor abilities determined computationally. This information can be used to predict when hydride transfer reactions between transition-metal complexes and three-coordinate boron compounds should occur and what the driving force for these reactions should be. The use of this extensive scale of hydride donor abilities for transition-metal hydrides and BX$_3$ compounds is illustrated with a few selected reactions relevant to the regeneration of AB.

**Thermodynamic Studies of [(H)$_2$Rh(dmpe)$_2$][CF$_3$SO$_3$].** Previously, we studied the reactions of H$_2$ with [Rh(dmpe)$_2$][CF$_3$SO$_3$] and [Rh(depe)$_2$][CF$_3$SO$_3$], (depe = 1,2-bis(diethylphosphinoethane)) as shown on the left in reaction 2, and determined equilibrium constants of 2.1 ± 0.1 atm$^{-1}$ and 0.23 ± 0.02 atm$^{-1}$, respectively, using acetonitrile as the solvent.[12] Reactions of [Rh(dmpe)$_2$][CF$_3$SO$_3$] with H$_2$ in the presence of strong bases provided a qualitative measure of the acidity of [(H)$_2$Rh(dmpe)$_2$]$^+$. For example, potassium *tert*-butoxide (p$K_a$ *tert*-butanol = 32.2 in Me$_2$SO),[13] deprotonates [(H)$_2$Rh(dmpe)$_2$]$^+$, establishing an equilibrium between [(H)$_2$Rh(dmpe)$_2$]$^+$ and HRh(dmpe)$_2$. This result indicated that the acidity of [(H)$_2$Rh(dmpe)$_2$]$^+$ was low and quantitative p$K_a$ measurements of [(H)$_2$Rh(dmpe)$_2$]$^+$ would require base strengths greater than 30 p$K_a$ units in acetonitrile. Ideally, measurements of this type should be performed in acetonitrile, where a large body of comparative data is available and the effects of ion-pairing and self-association can be minimized.[14] Unfortunately, it was not possible to measure p$K_a$ values of these complexes in acetonitrile or benzonitrile, due to undesirable side reactions of HRh(dmpe)$_2$ and HRh(depe)$_2$ with these solvents. After surveying several bases, we found that the isopropyl derivative of Verkade's base (VSB-$^i$pr) (P(RNCH$_2$CH$_2$)$_3$N, R = $^i$Pr), a proazaphosphatrane nonionic superbase, was capable of meeting our requirements. It is sufficiently basic (p$K_a$ of 33.6 in acetonitrile[15]), the protonated and unprotonated forms of the base exhibit complete solubility in THF, and the bulky isopropyl groups surrounding the basic phosphorus site should minimize self-association between protonated and unprotonated forms of the base.

---

(7) (a) Berning, D. E.; Noll, B. C.; DuBois, D. L. *J. Am. Chem. Soc.* **1999**, *121*, 11432. (b) Curtis, C. J.; Miedaner, A.; Ellis, W. W.; DuBois, D. L. *J. Am. Chem. Soc.* **2002**, *124*, 1918.

(8) (a) Price, A. J.; Ciancanelli, R.; Noll, B. C.; Curtis, C. J.; DuBois, D. L.; DuBois, M. R. *Organometallics* **2002**, *21*, 4833. (b) Miedaner, A.; Raebiger, J. W.; Curtis, C. J.; Miller, S. M.; DuBois, D. L. *Organometallics* **2004**, *23*, 2670.

(9) Berning, D. E.; Miedaner, A.; Curtis, C. J.; Noll, B. C.; DuBois, M. R.; DuBois, D. L. *Organometallics* **2001**, *20*, 1832.

(10) Raebiger, J. W.; Miedaner, A.; Curtis, C. J.; Miller, S. M.; DuBois, D. L. *J. Am. Chem. Soc.* **2004**, *126*, 5502.

(11) Curtis, C. J.; Miedaner, A.; Raebiger, J. W.; DuBois, D. L. *Organometallics* **2004**, *23*, 511.

(12) DuBois, D. L.; Blake, D. M.; Miedaner, A.; Curtis, C. J.; DuBois, M. R.; Franz, J. A.; Linehan, J. C. *Organometallics* **2006**, *25*, 4414.

(13) Olmstead, W. N.; Margolin, Z.; Bordwell, F. G. *J. Org. Chem.* **1980**, *45*, 3295.

(14) Jordan, R. F.; Norton, J. R. *J. Am. Chem. Soc.* **1982**, *104*, 1255.

(15) Kisanga, P. B.; Verkade, J. G. *J. Org. Chem.* **2000**, *65*, 5431.

(16) Qi, X.-J.; Liu, L.; Fu, Y.; Guo, Q.-X. *Organometallics* **2006**, *25*, 5879.

(17) Wayner, D. D. M.; Parker, V. D. *Acc. Chem. Res.* **1993**, *26*, 287.

(18) Qi, X.-J.; Fu, Y.; Liu, L.; Guo, Q.-X. *Organometallics* **2007**, *26*, 4197.

(19) Raebiger, J. W.; DuBois, D. L. *Organometallics* **2005**, *24*, 110.

(20) Grant, D. J.; Dixon, D. A.; Camaioni, D. M.; Potter, R. G.; Christe, K. O. *Inorg. Chem.* **2009**, DOI: 10.1021/ic901092x.

(21) Baker, R. T.; Ovenall, D. W.; Harlow, R. L.; Westcott, S. A.; Taylor, N. J.; Marder, T. B. *Organometallics* **1990**, *9*, 3028.

(22) Marder, T. B.; Williams, I. D. *J. Chem. Soc., Chem. Commun.* **1987**, 1478.

(23) Marks, T. J.; Kolb, J. R. *Chem. Rev.* **1977**, *77*, 263.

(24) A search of the 2008 Cambridge Structural Data Center (CSDC) revealed two coordinatively unsaturated metal complexes containing an outer sphere, non-coordinating BH$_4$ anion: (a) Antsyshkina, A. S.; Porai-Koshits, M. A.; Makhaev, V. D.; Borisov, A. P.; Mal'tseva, N. N. *Koord. Khim.* **1992**, *18*, 474. (b) Burgess, K.; van der Donk, W. A.; Westcott, S. A.; Marder, T. B.; Baker, R. T.; Calabrese, J. C. *J. Am. Chem. Soc.* **1992**, *114*, 9350.

(25) Elliot, J. R.; Boldebuck, E. M.; Roedel, G. F. *J. Am. Chem. Soc.* **1952**, *74*, 5047.

(26) Schlesinger, H. I.; Brown, H. C.; Gilbreath, J. R.; Katz, J. J. *J. Am. Chem. Soc.* **1953**, *75*, 195.

(27) VanPaasschen, J. M.; Geanangel, R. A. *J. Am. Chem. Soc.* **1972**, *94*, 2680.

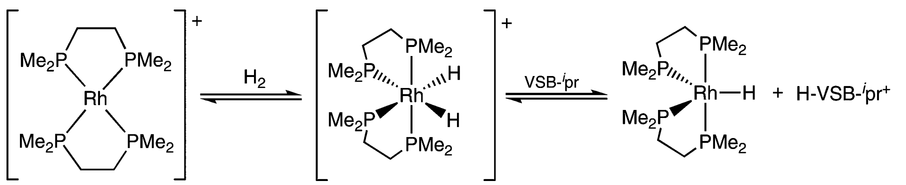

(2)

Upon bubbling $H_2$ through a solution of $[Rh(dmpe)_2]$-$[CF_3SO_3]$ in the presence of excess VSB-$^i$pr, an equilibrium was observed in THF (shown on right in reaction 2). This reaction was monitored by $^{31}P$ NMR spectroscopy and resonances corresponding to $[(H)_2Rh(dmpe)_2]^+$ and $HRh(dmpe)_2$ were integrated to determine the ratios of these two products. These ratios were used to calculate an equilibrium constant of $(1.2 \pm 0.3) \times 10^{-3}$. Assuming that this equilibrium constant in THF is a reasonable estimate of the equilibrium constant in acetonitrile, a p$K_a$ value of 36.5 can be calculated for $[(H)_2Rh(dmpe)_2][CF_3SO_3]$ in acetonitrile. The assumption of nearly equivalent equilibrium constants for THF and acetonitrile solutions should be reasonable given that there is no net change in the charge of the species from one side of the equilibrium to the other and that the rhodium cation and the cationic protonated base are of similar size. Because of the limited choices of solvents available for this reaction, this p$K_a$ value for $[(H)_2Rh(dmpe)_2]^+$ in acetonitrile provides the best possible experimental value available to us at the present time. This value is in good agreement with the computationally derived p$K_a$ value of 36.7 determined by Liu and co-workers[16] in a study that developed an ab initio protocol to predict the p$K_a$ values of transition-metal hydride complexes in acetonitrile.

**Hydride Donor Ability of $HRh(dmpe)_2$ and $[HBEt_3]^-$.** The hydride donor ability of $HRh(dmpe)_2$ can be determined using reactions 3−5. Reaction 3 is the protonation of $HRh(dmpe)_2$ to form $[(H)_2Rh(dmpe)_2]^+$. The free energy associated with this reaction is −50.0 kcal/mol ($-1.37 \times pK_a$). Reaction 4, loss of $H_2$ from $[(H)_2Rh(dmpe)_2][CF_3SO_3]$, is the reverse of the $H_2$ addition reaction discussed above, and the free energy associated with this reaction is +0.4 kcal/mol ($RT \ln K_{H2}$). Reaction 5 is the heterolytic cleavage of $H_2$ gas to form $H^+$ and $H^-$ solvated in acetonitrile. The free energy of this reaction is +76.0 kcal/mol.[17] The sum of reactions 3−5 is reaction 6, the heterolytic cleavage of the Rh−H bond of $HRh(dmpe)_2$ to form $[Rh(dmpe)_2]^+$ and $H^-$. The free energy of reaction 6 ($\Delta G°_{H^-}$) is 26.4 kcal/mol, the sum of the free energies associated with reactions 3−5 (eq 7). This experimentally derived value is comparable to the computationally determined hydricity ($\Delta G°_{H^-}$) of 23.6 calculated for $HRh(dmpe)_2$ by Liu and co-workers.[18] To determine the hydride donor ability of $HRh(depe)_2$ we refer to a previous study[12] where the equilibrium constant for diphosphine ligand exchange reactions between $HRh(dmpe)_2$ and $HRh(depe)_2$ was determined. This measurement indicated that $HRh(dmpe)_2$ is a better hydride donor than $HRh(depe)_2$ by 1.7 kcal/mol. On the basis of this information, the free energy for the heterolytic cleavage of the Rh−H bond of $HRh(depe)_2$ to form $[Rh(depe)_2]^+$ and $H^-$ is 28.1 kcal/mol. As a check on this value, the hydride donor abilities of $HRh(depx)_2$ (45 kcal/mol)[19] and $[HPd(depx)_2]^+$ (61 kcal/mol)[10] (depx = 1,2-$(Et_2PCH_2)_2C_6H_4$) differ by 16 kcal/mol. A similar difference would be expected between $HRh(depe)_2$ and $[HPd(depe)_2]^+$, for which a value of 43 kcal/mol has been determined.[9] On this basis we would estimate a value of 27 kcal/mol for $\Delta G°_{H^-}$ for $HRh(depe)_2$, in good agreement with our measured value of 28.1 kcal/mol.

$$HRh(dmpe)_2 + H^+ \rightleftarrows [(H)_2Rh(dmpe)_2]^+ \tag{3}$$

$$[(H)_2Rh(dmpe)_2]^+ \rightleftarrows [Rh(dmpe)_2]^+ + H_2 \tag{4}$$

$$H_2 \rightarrow H^+ + H^- \tag{5}$$

$$HRh(dmpe)_2 \rightarrow [Rh(dmpe)_2]^+ + H^- \tag{6}$$

$$\Delta G^{o}_{H^-} - 1.37pK_a + \Delta G_{H2} + 76.0 \tag{7}$$

As noted above, we reported that $HRh(dmpe)_2$ has a hydride donor ability equal to that of $Li[HBEt_3]$, more commonly known as Super-Hydride.[12] This result was based on $^1H$ NMR spectral data indicating the formation of an equilibrium between $[HBEt_3]^-$ and $BEt_3$ upon titrating $HRh(dmpe)_2$ with $BEt_3$. These results were corroborated by the disappearance of $HRh(dmpe)_2$ and the simultaneous formation of $[Rh(dmpe)_2]^+$ in the $^{31}P$ NMR spectrum. Furthermore, when $Li[HBEt_3]$ was added to $[Rh(dmpe)_2][CF_3SO_3]$, $HRh(dmpe)_2$ and $[Rh(dmpe)_2][CF_3SO_3]$ were observed by $^{31}P$ NMR, as expected for a true equilibrium. These results indicate that the hydride donor ability of $Li[HBEt_3]$ should be approximately 26 kcal/mol on the acetonitrile hydride donor scale.

**Determination of Hydride Affinities of $BX_3$ Compounds.** To determine the relative hydride acceptor abilities or hydride affinities of $BX_3$ compounds, we performed electronic structure calculations on the isodesmic reaction of $BX_3$ with $[HBEt_3]^-$, shown in reaction 8.

$$HBEt_3^- + BX_3 \xrightarrow{\Delta H°} BEt_3 + HBX_3^- \tag{8}$$

We follow the convention where the gas-phase hydride affinity is defined as the negative of the $\Delta H°$ value for addition of $H^-$ to a molecule in the gas-phase. The hydride affinity of $BH_3$ is known from accurate calculations[20] to be 73.7 kcal/mol. From this value and $\Delta H° = -15.5$ calculated for the hydride transfer from $[HBEt_3]^-$ to $BH_3$, we estimate the hydride affinity of $BEt_3$ to be 58.2 kcal/mol in the gas-phase. Our results show that the hydride affinity for $BX_3$ compounds varies over a wide range, depending on the nature of X. Table 1 summarizes the computationally derived gas-phase hydride affinity values for the $BX_3$ compounds used

***Table 1.*** Hydride Affinity Values of $BX_3$ Compounds Calculated Using the B3LYP/6-311+G** Level of Theory

| $BX_3$ compound | hydride affinity $-\Delta H°$ (kcal/mol) |
|---|---|
| $B(O^tBu)_3$ | 38.0 |
| $B(OSiMe_3)_3$ | 46.4 |
| $BEt_3$ | 58.2 |
| $B(SMe)_3$ | 69.0 |
| $B(p\text{-}OC_6H_4OMe)_3$ | 69.9 |
| $BH_3$ | 73.7 |
| $B(OPh)_3$ | 74.0 |
| $HB(S_2C_6H_4)$ | 74.3 |
| $BF_3$ | 75.5 |
| $B(SPh)_3$ | 86.9 |
| $B(OC_6F_5)_3$ | 94.3 |

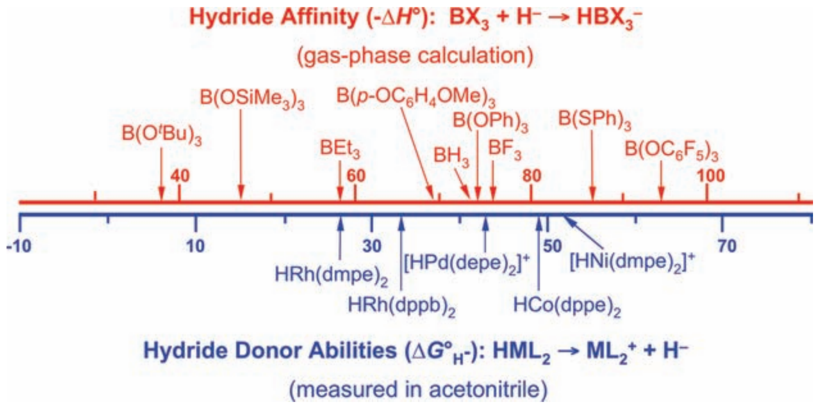

***Figure 1.*** Scales of experimentally determined hydride donor abilities of selected transition-metal hydride complexes in acetonitrile (blue, bottom) and the calculated gas-phase hydride affinity values for selected $BX_3$ compounds (red, top).

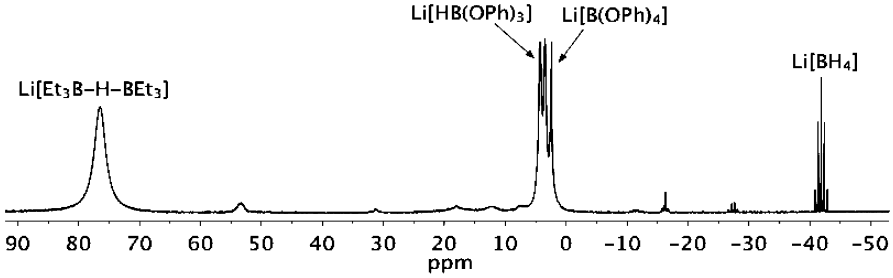

***Figure 2.*** $^1H$-coupled $^{11}B$ NMR spectrum of the reaction between $Li[HBEt_3]$ and $B(OPh)_3$ recorded immediately after mixing.

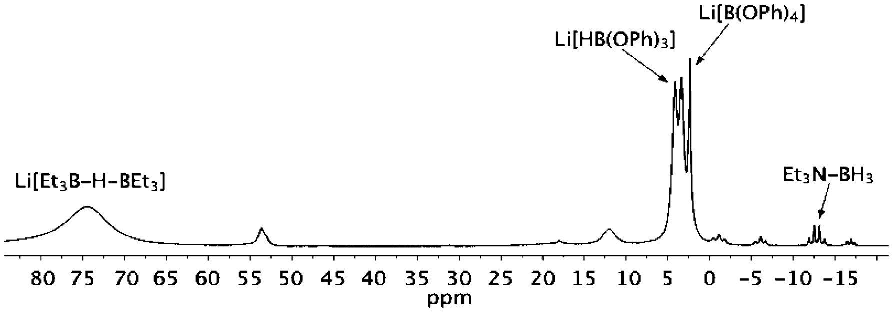

***Figure 3.*** $^1H$-coupled $^{11}B$ NMR spectrum of the reaction between $Li[HBEt_3]$ and $B(OPh)_3$ in a 10% $NEt_3 \cdot THF$ mixture recorded after heating at 50 °C for 5 h.

in this study. Because $HRh(dmpe)_2$ and $[HBEt_3]^-$ have the same hydride donor abilities, it is possible to relate these two scales as shown in Figure 1, assuming constant $T\Delta S$ and solvent corrections. This quantitative approach to examining hydride transfer reactions predicts that $HRh(dmpe)_2$ and $Li[HBEt_3]$ have the ability to transfer a hydride ligand to $BX_3$ compounds with hydride affinities greater than 58 kcal/mol. In accord with this result, the selected transition-metal hydrides included in Figure 1 should have the ability to transfer a hydride ligand to $BX_3$ compounds located to the right of their position on the parallel hydride affinity scale.

**Hydride Transfer Reactions from Triethylborohydride to Borate Esters, $B(OR)_3$ (R = $^t$Bu, Ph).** To determine whether the calculated gas-phase hydride affinities may be useful in predicting hydride transfer in solution between boron compounds, we performed reactions of the subject borate esters with $Li[HBEt_3]$. The reagents were mixed in THF, and the reaction was monitored by $^{11}B$ NMR spectroscopy. $B(O^tBu)_3$, the poorest hydride acceptor of the $BX_3$ compounds in this study, does not accept a hydride even with a 10-fold excess of $Li[HBEt_3]$. This result is consistent with the calculated large positive enthalpy change ($\Delta H_r^\circ$ = 20 kcal/mol) of this reaction. In contrast, $B(OPh)_3$ readily accepts hydride from $Li[HBEt_3]$ even when less than stoichiometric amounts of hydride are used, consistent with the calculated large negative enthalpy change ($\Delta H_r = -16$ kcal/mol) of this reaction. Figure 2 shows the $^1H$-coupled $^{11}B$ NMR spectrum of the reaction mixture, indicating that $Li[HB(OPh)_3]$ is formed as well as products of ligand redistribution, $Li[B(OPh)_4]$ and $Li[BH_4]$. Furthermore, as shown by the $^1H$-coupled $^{11}B$ NMR spectrum in Figure 3, when the reaction is carried out in the presence of triethylamine, a small amount of $Et_3N\text{-}BH_3$ is formed instead of $Li[BH_4]$.

**Hydride Transfer Reactions from Rhodium to Borate Esters $B(OR)_3$ (R = Ph, $C_6F_5$, $p$-$C_6H_4OMe$, $Si(CH_3)_3$, $^t$Bu).** To validate that the juxtaposition of the hydride affinity and hydride donor ability scales shown in Figure 1 is correct, the reactions between $HRh(dmpe)_2$ and selected $B(OR)_3$ compounds were performed in THF, according to reaction 9 where $n$ = 0, 2, or 3.

$$HRh(dmpe)_2 + B(OR)_3 \xrightarrow{THF} [Rh(dmpe)_2][HB(OR)_3] + [Rh(dmpe)_2][H_nB(OR)_{4-n}] \quad (9)$$

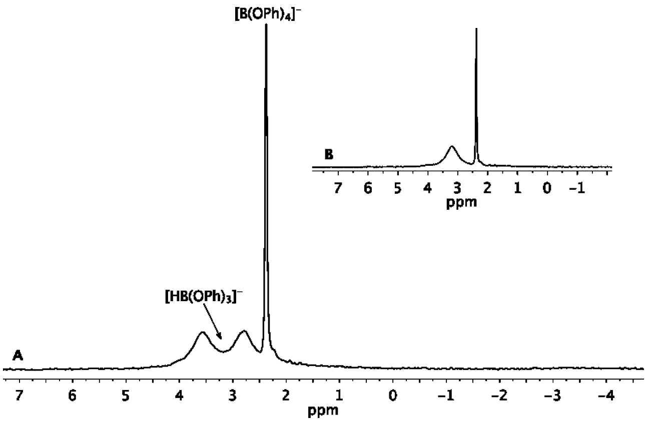

***Figure 4.*** (A) $^1$H-coupled $^{11}$B NMR spectrum recorded at 50 °C from the hydride transfer reaction of HRh(dmpe)$_2$ to B(OPh)$_3$. (B) The corresponding $^{11}$B{$^1$H} NMR spectrum recorded at 50 °C.

***Table 2.*** $^{11}$B NMR Data for Products Formed via Hydride Transfer from HRh(dmpe)$_2$

| M = [Rh(dmpe)$_2$]$^+$ | $^{11}$B NMR $\delta$ (ppm) | $J_{B-H}$ (Hz) |
|---|---|---|
| M[HB(OPh)$_3$] | 3.2 | 124 |
| M[B(OPh)$_4$] | 2.4 | – |
| M[HB(OC$_6$F$_5$)$_3$] | 5.0 | 137 |
| M[HB($p$-OC$_6$H$_4$OMe)$_3$] | 3.8 | 105 |
| M[BH$_4$] | −37.4 | 82 |
| Et$_3$N-BH$_2$F | 3.0 | 114 |
| M[H$_2$B(S$_2$C$_6$H$_4$)] | −11.5 | 110 |
| M[HB(SPh)$_3$] | −4.3 | 128 |
| M[H$_2$B(SPh)$_2$] | −14.5 | 111 |
| M[H$_3$B(SPh)] | −25.6 | 97 |
| M[B(SPh)]$_4$ | 4.5 | – |
| Et$_3$N-BH$_2$(SPh) | −6.5 | 115 |
| H$_3$B-NEt$_3$ | −12.8 | 96 |

Experimental results support the computational studies suggesting that hydride transfer reactions are thermodynamically favorable for boron compounds with calculated hydride affinities greater than 58 kcal/mol. For example, the room temperature reaction performed in THF between excess HRh(dmpe)$_2$ and B(OPh)$_3$, with a hydride affinity of 74 kcal/mol, was monitored by $^{31}$P NMR spectroscopy. Consumption of HRh(dmpe)$_2$, (d, $\delta$ 26.5, $^1J_{RhP} = 139$ Hz) via hydride transfer, was indicated by clean conversion to [Rh(dmpe)$_2$]$^+$, as indicated by $^{31}$P{$^1$H} NMR spectroscopy (d, $\delta$ 36.0, $^1J_{RhP} = 125$ Hz, identical to [Rh(dmpe)$_2$][CF$_3$SO$_3$]). The $^{11}$B{$^1$H} NMR spectrum recorded at 50 °C, (Figure 4, trace B) displays two major boron-containing products, a sharp singlet at $\delta$ 2.4 and a broad singlet at $\delta$ 3.2. The sharp singlet is assigned to [Rh(dmpe)$_2$][B(OPh)$_4$] based on an X-ray diffraction and $^{11}$B{$^1$H} NMR study of crystals that precipitated from the reaction (see Figure S5 in the Supporting Information). In the $^1$H-coupled $^{11}$B NMR spectrum shown in trace A of Figure 4, the resonance at $\delta$ 3.2 is a broad doublet ($^1J_{BH} = 124$ Hz), confirming the formation of a B−H bond. On the basis of this chemical shift, the B−H coupling constant, and a B−H stretching frequency of 2350 cm$^{-1}$ (KBr), the second product is attributed to the formation of [Rh(dmpe)$_2$][HB(OPh)$_3$]. Table 2 summarizes the $^{11}$B chemical shifts and B−H coupling constants for products formed via hydride transfer reactions described in this study. The reaction mixture described here and those discussed in the following sections are generally stable for several days if stored in an oxygen- and water-free environment. The independent synthesis of Li[HB(OPh)$_3$] and further discussion of the $^{11}$B chemical shifts for this complex are provided in the Supporting Information.

As indicated by the examples in Table 1, the substitution of electron-donating or electron-withdrawing functionalities on the aryl rings can dramatically alter the hydride affinity of the BX$_3$ compound. In addition to B(OPh)$_3$, selected B(OR)$_3$ compounds, reflecting a wide range of hydride affinity values, were examined. Hydride transfer reactions between excess HRh(dmpe)$_2$ and the borate esters B(OC$_6$F$_5$)$_3$ and B($p$-OC$_6$H$_4$OMe)$_3$ resulted in similar B−H-containing products, while experiments conducted using excess HRh(dmpe)$_2$ with the borate esters B(OSi(Me)$_3$)$_3$ and B(O$^t$Bu)$_3$, provided no spectroscopic evidence of hydride transfer even after heating at 50 °C for 3 days. Notably, the formation of [B(OR)$_4$]$^-$ was routinely encountered as a major reaction product, likely resulting from redistribution of the aryloxy group. Hydride transfer does not occur between HRh(dmpe)$_2$ and [B(OAr)$_4$]$^-$, highlighting the stability of the four-coordinate borate ester. A description of these reactions and discussion regarding [B(OAr)$_4$]$^-$ formation is included in the Supporting Information.

**Hydride Transfer Reactions from Rhodium to Borane−THF.** We previously reported that attempts to synthesize HRh(dmpe)$_2$ by treatment of [Rh(dmpe)$_2$][CF$_3$SO$_3$] with bis(triphenylphosphine)iminium borohydride (PPNBH$_4$) in THF were unsuccessful.[12] This indicated that the tetrahydroborate anion is not sufficiently hydridic to transfer a hydride ligand to rhodium, and that the reverse reaction, hydride transfer to BH$_3$·THF from HRh(dmpe)$_2$, should be thermodynamically favorable. The hydride affinity of BH$_3$ is 73.7 kcal/mol,[20] similar to the value for B(OPh)$_3$. A $^{11}$B{$^1$H} NMR spectrum taken after the addition of a 1.0 M BH$_3$·THF solution to HRh(dmpe)$_2$ in THF results in the formation of a singlet observed at $\delta$ −37.4. The $^1$H-coupled $^{11}$B NMR spectrum reveals the expected quintet for the tetrahydroborate anion assigned as [Rh(dmpe)$_2$][BH$_4$], (see Figure S8 in the Supporting Information). A notable example of a similar hydride transfer reaction was reported by Baker and co-workers where HRh(dmpe)$_2$ reacts with 0.5 equiv of thexylborane ([BH(CMe$_2$CHMe$_2$)($\mu$-H)]$_2$) via hydride transfer to produce [Rh(dmpe)$_2$][H$_3$B(thexyl)] as determined by NMR spectroscopy.[21] In addition to hydride transfer product [Rh(dmpe)$_2$][BH$_4$], a competing reaction is frequently observed, especially when excess quantities of BH$_3$·THF are added to HRh(dmpe)$_2$, resulting in the formation of dmpe-(BH$_3$)$_2$. This side reaction can be attenuated by the addition of substoichiometric amounts of BH$_3$·THF. Crystals of [Rh(dmpe)$_2$][BH$_4$] suitable for an X-ray diffraction study were grown from a concentrated THF solution. The molecular structure of [Rh(dmpe)$_2$][BH$_4$], shown in Figure 5, contains a square-planar cation formed by rhodium and two dmpe ligands. The presence of discrete uncoordinated tetrahydroborate anions as the counterion to the [Rh(dmpe)$_2$]$^+$ cations confirm that hydride transfer from rhodium to boron has occurred. The [Rh(dmpe)$_2$]$^+$ cation contains typical Rh−P bond distances of 2.274(2) and 2.287(2) Å analogous to literature reports.[22] The four hydrogen atoms of the tetrahydroborate anion were located in the difference Fourier map. Selected bond lengths and bond angles are listed in Table 3. Tetrahydroborate ions commonly form covalent $\sigma$-complexes through bridging hydrogen atoms with a variety of transition metals.[23] This can be especially common for complexes that are coordinatively unsaturated such as [Rh(dmpe)$_2$]$^+$. However, this is a rare example[24] where the molecular structure of [Rh-

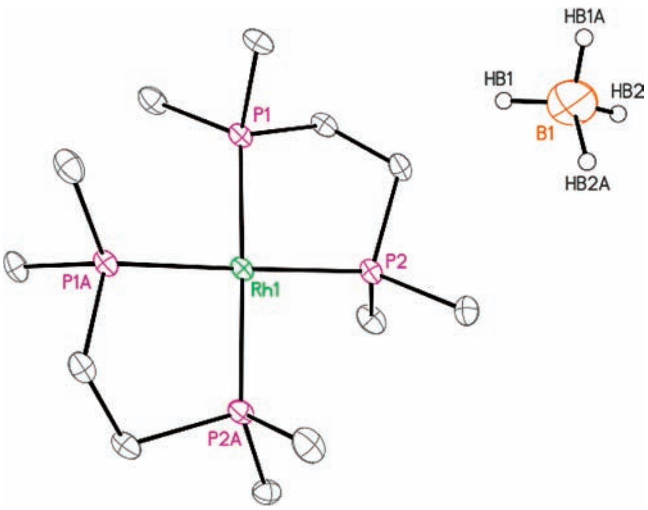

***Figure 5.*** Molecular structure of [Rh(dmpe)$_2$][BH$_4$] with atom numbering. Thermal ellipsoids drawn at 30% probability. Hydrogen atoms omitted except on the BH$_4$ anion.

***Table 3.*** Selected Bond Distances (Å) and Angles (deg) for [Rh(dmpe)$_2$][BH$_4$], *trans*-[HRh(SPh)(dmpe)$_2$][HB(SPh)$_3$], and [Rh(dmpe)$_2$][SPh]

| | | | |
|---|---|---|---|
| | [Rh(dmpe)$_2$][BH$_4$] | | |
| Rh(1)−P(1) | 2.2737 (17) | P(1)−Rh(1)−P(2) | 83.97 (6) |
| Rh(1)−P(2) | 2.2870 (17) | P(1)−Rh(1)−P(1A) | 95.73 (9) |
| B(1)−H1 | 1.04 (4) | P(1)−Rh(1)−P(2A) | 177.78 (7) |
| B(1)-H2 | 1.04 (3) | HB1−B(1)−HB2 | 111 (5) |
| | *trans*-[HRh(SPh)(dmpe)$_2$][HB(SPh)$_3$] | | |
| Rh(1)−P(1) | 2.3206 (4) | P(1)−Rh(1)−P(2) | 84.580 (12) |
| Rh(1)−P(2) | 2. 3209 (3) | P(1)−Rh(1)−P(3) | 95.109 (12) |
| Rh(1)−P(3) | 2.3224 (3) | P(1)−Rh(1)−P(4) | 176.691 (12) |
| Rh(1)−P(4) | 2.3144 (3) | P(2)−Rh(1)−P(3) | 167.956 (11) |
| Rh(1)−S(1) | 2.5083 (4) | P(2)−Rh(1)−P(4) | 95.167 (12) |
| Rh(1)−H | 1.492 (18) | P(3)−Rh(1)−P(4) | 84.447 (12) |
| B(1)−S(2) | 1.9345 (17) | P(1)−Rh(1)−S(1) | 92.901 (12) |
| B(1)−S(3) | 1.9162 (16) | P(2)−Rh(1)−S(1) | 105.080 (11) |
| B(1)−S(4) | 1.9122 (16) | S(1)−Rh(1)−H(1R) | 172.1 (7) |
| B(1)−H | 1.05 (2) | S(2)−B(1)−S(3) | 107.60 (8) |
| | | S(2)−B(1)−S(4) | 117.79 (8) |
| | | S(3)−B(1)−S(4) | 108.21 (8) |
| | | S(2)−B(1)−HB(1) | 110.0 (11) |
| | [Rh(dmpe)$_2$][SPh] | | |
| Rh(1)−P(1) | 2.2797 (5) | P(1)−Rh(1)−P(2) | 84.43 (2) |
| Rh(1)−P(2) | 2.2767 (5) | P(1)−Rh(1)−P(2A) | 177.663 (19) |
| Rh(2)−P(3) | 2.2898 (5) | P(1)−Rh(1)−P(1A) | 95.60 (3) |
| Rh(2)−P(4) | 2.2884 (5) | P(3)−Rh(2)−P(4) | 84.384 (17) |
| S(1)−C(18) | 1.740 (2) | P(3)−Rh(2)−P(3A) | 179.998 (18) |
| | | P(3)−Rh(2)−P(4A) | 95.614 (17) |

(dmpe)$_2$][BH$_4$] clearly indicates the tetrahydroborate anion resides in the outer sphere and does not interact with the rhodium center.

**Hydride Transfer Reactions from Rhodium to BF$_3$·OEt$_2$.** Early work of Schlesinger and Brown[25,26] discovered that diborane could be prepared in high yields by the reaction of lithium or sodium hydride with boron trifloride diethyletherate. To determine if analogous reactivity was possible using transition-metal hydrides, we investigated the reaction between HRh(dmpe)$_2$ and BF$_3$·OEt$_2$ in THF in the presence of triethylamine in order to intercept Et$_3$N-BH$_3$. The hydride affinity for BF$_3$ was calculated to be 76 kcal/mol, slightly greater than the value for BH$_3$, indicating favorable thermochemistry for hydride transfer from HRh(dmpe)$_2$. BF$_3$·OEt$_2$ was added to excess HRh(dmpe)$_2$ and NEt$_3$ in THF, and the solution was heated at 50 °C for one hour. Examination of the $^1$H-coupled $^{11}$B NMR spectrum (trace A, Figure S9 in the Supporting Information) revealed a quartet at $\delta$ −12.8 ($J_{B-H}$ = 97 Hz), corresponding to Et$_3$N-BH$_3$, and a singlet at $\delta$ −1.1, indicating the formation of [Rh(dmpe)$_2$][BF$_4$] that slowly precipitates over the course of the reaction. In addition, the mixed species Et$_3$N-BH$_2$F[27] appears as an overlapping doublet of triplets at $\delta$ 3.0 ($J_{B-H}$ = 114 Hz), corroborated by a doublet ($J_{B-F}$ = 86 Hz) in the $^{11}$B{$^1$H} NMR spectrum. Gentle heating of the reaction mixture at 50 °C for 20 h leads to the disappearance of Et$_3$N-BH$_2$F and produces [Rh(dmpe)$_2$][BF$_4$] and Et$_3$N-BH$_3$ as the major boron species in solution (trace B of Figure S9, Supporting Information). Broad features at *ca.* $\delta$ 20 are assigned to species that are believed to be polymeric in nature and that are caused by the ring-opening of THF by BF$_3$ or other boron intermediates produced in the reaction.[28]

**Hydride Transfer Reactions from Rhodium to 1,3,2-benzodithiaborolane.** 1,2-Dithiobenzene has been used to digest the polymeric product resulting from dehydrogenation of AB to form the ammonia adduct of 1,3,2-benzodithiaborolane, (C$_6$H$_4$S$_2$)BH·(NH$_3$).[6] We were interested to see if HRh(dmpe)$_2$ would transfer a hydride ligand to a similar species, HB(S$_2$C$_6$H$_4$). The computed hydride affinity of 74 kcal/mol for HB(S$_2$C$_6$H$_4$) is nearly identical to that of B(OPh)$_3$, and therefore hydride transfer is expected. In fact, hydride transfer is observed upon mixing a 1:1 ratio of HRh(dmpe)$_2$ and HB(S$_2$C$_6$H$_4$) in THF. Initially this reaction produced a yellow precipitate in THF at room temperature; however, the $^1$H-coupled $^{11}$B NMR spectrum recorded at 50 °C exhibits a triplet at $\delta$ −11.5 ($J_{B-H}$ = 110 Hz) (Figure S6 in the Supporting Information), corresponding to the formation of [H$_2$B(S$_2$C$_6$H$_4$)]$^-$. This value is nearly identical to that of Li[H$_2$B(S$_2$C$_6$H$_4$)] (t, $\delta$ −11.0, $J_{B-H}$ = 110 Hz) reported by Nöth and co-workers prepared by the reaction of LiBH$_4$ with 1,2-dithiobenzene in THF.[29] Reactions performed with a 3-fold excess of HRh(dmpe)$_2$ produced identical results, suggesting the chelate effect of the dithiolate ligand precludes further B−H bond formation.

**Hydride Transfer Reactions from Rhodium to B(SPh)$_3$.** In the preceding discussion, the utility of the hydride affinity and hydride donor ability scales for predicting the feasibility of hydride transfer reactions was demonstrated. However, the inability of HRh(dmpe)$_2$ to reduce [B(OPh)$_4$]$^-$, [BF$_4$]$^-$, and [H$_2$B(S$_2$C$_6$H$_4$)]$^-$ by cleaving the B−O, B−F, and B−S bonds, respectively, limits the extent of conversion of these species. A second objective of this work was to demonstrate that transition-metal hydrides, such as HRh(dmpe)$_2$, could be used to generate boron compounds containing multiple B−H bonds by converting BX$_3$ to BH$_3$ derivatives in which all B−X bonds are cleaved. We hoped to achieve this by selecting BX$_3$ compounds with appropriate heterolytic B−X bond strengths. In this section, a series of reactions between HRh(dmpe)$_2$ and B(SPh)$_3$ are described that demonstrate the feasibility of forming boron products containing multiple B−H bonds (e.g., reaction 10, where $n$ = 2, 3, 4) *and* forming Et$_3$N-BH$_3$ in the presence of NEt$_3$.

---

(28) (a) Edwards, J. D.; Gerrard, W.; Lappert, M. F. *J. Chem. Soc.* **1957**, 348. (b) Gerrard, W.; Lappert, M. F. *Chem. Rev.* **1958**, *58*, 1081.

(29) Knizek, J.; Nöth, H. *J. Organomet. Chem.* **2000**, *614−615*, 168.

$$\mathrm{HRh(dmpe)_2} + \mathrm{B(SPh)_3} \xrightarrow{\mathrm{THF}} [\mathrm{Rh(dmpe)_2}][\mathrm{H}_n\mathrm{B(SPh)}_{4\text{-}n}] \qquad (10)$$

Hydride transfer reactions from $HRh(dmpe)_2$ to $B(SPh)_3$ are expected to be thermodynamically favorable on the basis of the hydride affinity of $B(SPh)_3$ of 87 kcal/mol. In addition, due to a weaker B−S bond[20] compared to B−O and B−F bonds, and absent the chelate effect, thiolate ligand substitution was anticipated to be facile, improving the likelihood of boron products with multiple B−H bonds and decreased $[B(SPh)_4]^-$ formation. Hydride transfer reactions of $HRh(dmpe)_2$ with $B(SPh)_3$ were performed in THF, resulting in rapid hydride transfer to boron as described below. Although reports describing aryl- and alkyl-transfer[30] between $H_2B(SPh)$ (a potential hydride transfer product) and ethereal solvents such as THF and diethyl ether have been noted, these types of side reactions were not observed in our studies.

Reactions of a slight excess of $B(SPh)_3$ with $HRh(dmpe)_2$ in THF were followed by $^{31}P$ and $^{11}B$ NMR spectroscopy. $^{31}P\{^1H\}$ spectral data indicated complete consumption of $HRh(dmpe)_2$, resulting in the formation of $[Rh(dmpe)_2]^+$ (d, $\delta$ 35.7, $^1J_{RhP}$ = 125 Hz) as the major phosphorus-containing product (Figure 6, trace B). In addition, a minor doublet located at $\delta$ 38.2, ($^1J_{RhP}$ = 90 Hz) was observed accounting for approximately 2% of the total product mixture by integration. This minor species was identified as *trans*-$[HRh(SPh)(dmpe)_2]^+$, and was prepared independently by the reaction of thiophenol with $[Rh(dmpe)_2][CF_3SO_3]$ to confirm the $^{31}P$ NMR spectral data. The formation of this six-coordinate rhodium species suggests trace amounts of thiophenol in the $B(SPh)_3$ oxidatively adds to $[Rh(dmpe)_2]^+$ after hydride transfer was complete. The $^1H$-coupled $^{11}B$NMR spectrum recorded at 50 °C immediately after mixing, shown by trace A of Figure 6, indicated the presence of three major boron-containing species, unreacted $B(SPh)_3$ at $\delta$ 62.3, a sharp resonance at $\delta$ 4.5 assigned to $[B(SPh)_4]^-$, and a doublet at $\delta$ −4.3 ($^1J_{BH}$ = 128 Hz) assigned to $[HB(SPh)_3]^-$, indicating the formation of a B−H bond.

Slow diffusion of ether into the reaction mixture precipitated a crop of yellow crystals accounting for the majority of the material. Unfortunately, these crystals were not suitable for X-ray diffraction studies. However, a minor component of this recrystallization was suitable for analysis by X-ray diffraction. The molecular structure of this material is shown in Figure 7. The cation of the colorless crystals is the octahedral rhodium(III) species, *trans*-$[HRh(SPh)(dmpe)_2]^+$, rather than the anticipated $[Rh(dmpe)_2]^+$. The rhodium coordination sphere consists of two dmpe ligands occupying the equatorial positions, while a thiophenolate ligand and a hydride ligand occupy the apical positions. The average Rh−P bond distance is 2.3196(3) Å, comparable to other octahedral Rh(III) complexes with chelating phosphine ligands.[31] The Rh−S bond length is long at 2.5083(4) Å, while the Rh−H bond length is 1.49(2) Å. The identity of the anion supports our assignment of the upfield doublet as $[HB(SPh)_3]^-$. The geometry of $[HB(SPh)_3]^-$ can be regarded as nearly tetrahedral about the boron center, compared to the planar geometry of three-coordinate boron in the molecular structure of $B(SPh)_3$ (see Figure S7 in the Supporting Information). Two of the thiophenolate ligands are endo with respect to the hydride ligand, while the third thiophenolate ligand is exo. The B−S bond lengths of the $[HB(SPh)_3]^-$ anion are 1.916(2), and 1.935(2) Å and 1.912(2), respectively, while the B−H bond length is 1.05(2) Å. These B−S bond distances are slightly longer than the average of the B−S bond distances in $B(SPh)_3$ (1.80 Å). Selected metric parameters are listed in Table 3. The molecular structures determined for $B(SPh)_3$ and $[HB(SPh)_3]^-$ by X-ray diffraction are consistent with the optimized molecular structures of these compounds determined computationally.

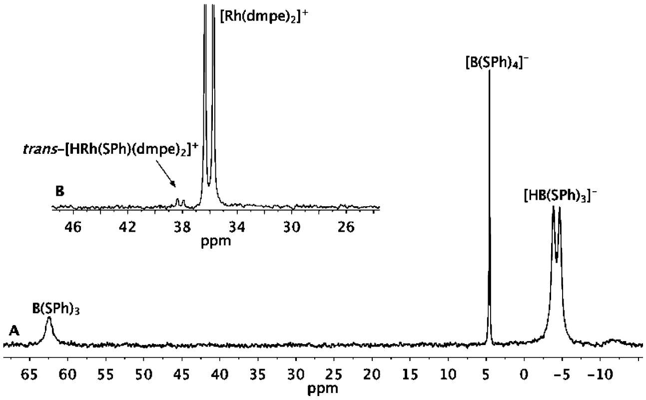

***Figure 6.*** (A) $^1H$-coupled $^{11}B$ NMR spectrum recorded at 50 °C of the reaction between excess $B(SPh)_3$ and $HRh(dmpe)_2$. (B) The corresponding $^{31}P\{^1H\}$ NMR spectrum.

Hydride transfer reactions performed with an excess of $HRh(dmpe)_2$ produced significantly different results. The $^1H$-coupled $^{11}B$ NMR spectrum recorded immediately after mixing a 3:1 ratio of $HRh(dmpe)_2$ to $B(SPh)_3$ is shown in Figure 8, trace A. Similar to the reaction using a 1:1 ratio, $[HB(SPh)_3]^-$ and $[B(SPh)_4]^-$ are observed at $\delta$ −4.3 and $\delta$ 4.5, respectively. However, a new triplet is present in this reaction at $\delta$ −14.5, $J_{B-H}$ = 111 Hz, assigned to $[H_2B(SPh)_2]^-$, indicating the formation of two B−H bonds. The chemical shift of $[H_2B(SPh)_2]^-$ is similar to that reported for $Li[H_2B(S_2C_6H_4)]$, *vide supra*. Integration of the corresponding $^{31}P$ NMR spectrum indicates roughly one-half of $HRh(dmpe)_2$ was consumed producing $[Rh(dmpe)_2]^+$ as the only observable phosphorus-containing product. The reaction mixture was heated at 50 °C for 30 min and the $^{31}P$ and $^{11}B$ spectral data were recorded once again. The $^1H$-coupled $^{11}B$ NMR spectrum recorded at 50 °C, Figure 8, trace B revealed the reaction mixture had significantly changed. The products $[B(SPh)_4]^-$ and $[HB(SPh)_3]^-$ ($\delta$ −4.3) were not observed and the reaction contained only $[H_2B(SPh)_2]^-$ (t, $\delta$ −14.5) and a new quartet at $\delta$ −25.6, $J_{B-H}$ = 97 Hz assigned to $[H_3B(SPh)]^-$ with an integration ratio of 3:1. The $^{31}P$ NMR spectrum indicates ~ 85% of $HRh(dmpe)_2$ was consumed and $[Rh(dmpe)_2]^+$ was the only observed product. After heating the reaction at 50 °C for 20 h the $^{31}P$ NMR data indicated all of the $HRh(dmpe)_2$ was consumed. The corresponding $^1H$-coupled $^{11}B$ NMR spectrum, shown in Figure 8, spectrum C, indicates further changes in the boron-containing product distribution, suggesting additional B−H bonds have been formed. The amount of $[H_2B(SPh)_2]^-$ present after heating has decreased significantly and the major product is $[H_3B(SPh)]^-$, integrated at nearly a 1:5 ratio. In addition, two new products are observed, a complex multiplet centered at $\delta$ −38.8 and a quintet at $\delta$ −41.1 assigned to dmpe-$(BH_3)_2$ and $[BH_4]^-$,

---

(30) (a) Pasto, D. J. *J. Am. Chem. Soc.* **1962**, *84*, 3777. (b) Pasto, D. J.; Cumbo, C. C.; Balasubramaniyan, P. *J. Am. Chem. Soc.* **1966**, *88*, 2187.

(31) (a) Simonsen, K. P.; Suzuki, N.; Hamada, M.; Kojima, M.; Ohba, S.; Saito, Y.; Fujita, J. *Bull. Chem. Soc. Jpn.* **1989**, *62*, 3790. (b) Clegg, W.; Elsegood, M. R. J.; Scott, A. J.; Marder, T. B.; Dai, C.; Norman, N. C.; Pickett, N. L.; Robins, E. G. *Acta Crystallogr., Sect. C* **1999**, *55*, 733.

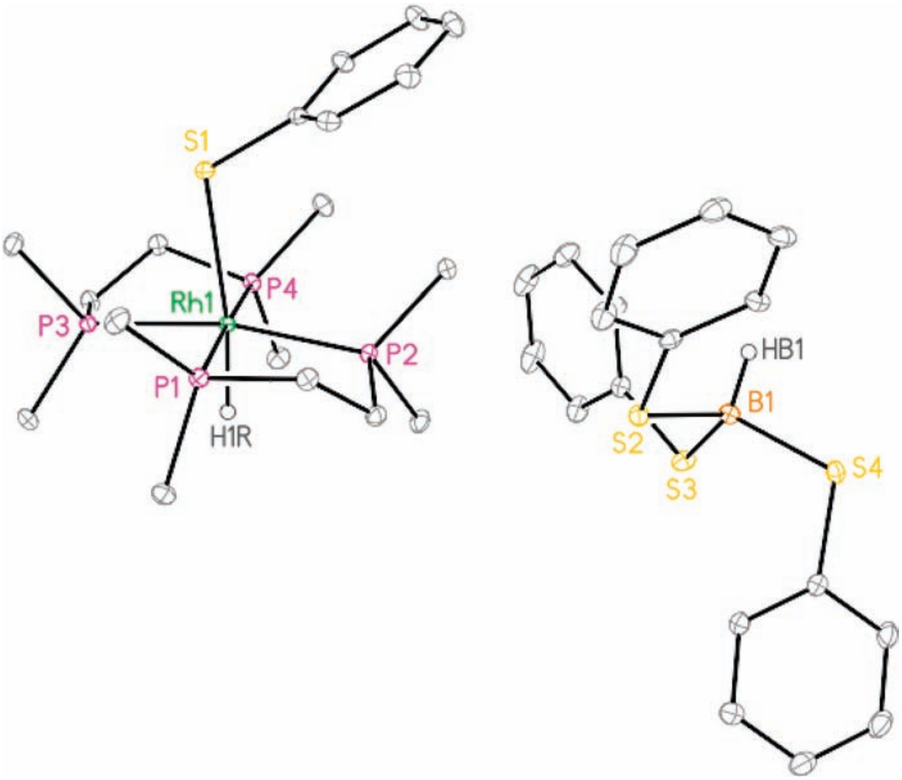

***Figure 7.*** Molecular structure of *trans*-[HRh(SPh)(dmpe)$_2$][HB(SPh)$_3$]·THF with atom numbering. Thermal ellipsoids drawn at 30% probability. The THF solvent molecule has been omitted as well as hydrogen atoms except for those bound to Rh and B.

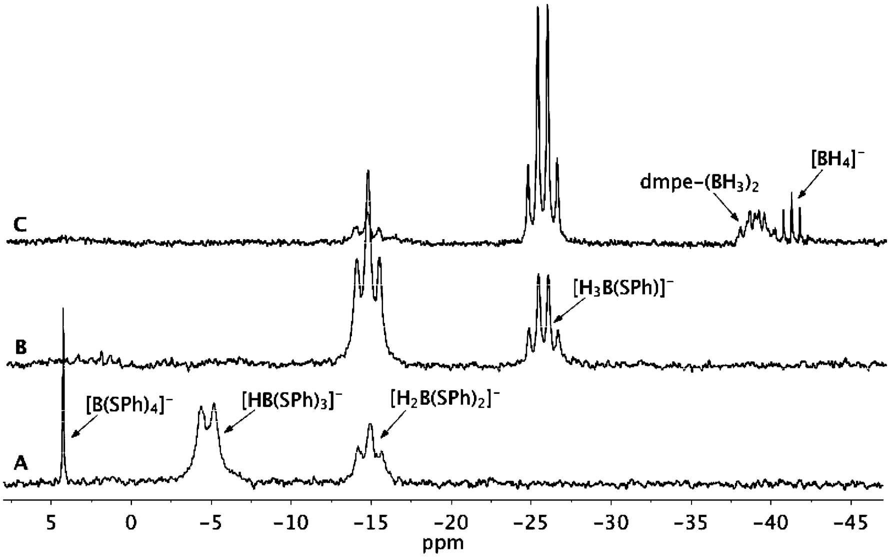

***Figure 8.*** $^1$H-coupled $^{11}$B NMR spectra from the hydride transfer reaction from HRh(dmpe)$_2$ to B(SPh)$_3$: (A) Immediately after mixing. (B) After heating at 50 °C, 30 min. (C) After heating at 50 °C, 20 h.

respectively. These results indicate that mild heating can produce the fully reduced tetrahydroborate anion, but also results in a slight decomposition of [Rh(dmpe)$_2$]$^+$. A possible decomposition pathway may involve the coordination of dmpe to BH$_3$ formed by dissociation of PhS$^-$ from [H$_3$B(SPh)]$^-$. A notable difference between reactions with B(SPh)$_3$ compared to B(OPh)$_3$ is the transitory formation of the [B(SPh)$_4$]$^-$ species. Reactions with B(OPh)$_3$ produce [B(OPh)$_4$]$^-$ as a final product, and hydride transfer to this species was not observed. Although [B(SPh)$_4$]$^-$ was formed in the initial stages of the reaction of B(SPh)$_3$ with excess HRh(dmpe)$_2$, [B(SPh)$_4$]$^-$ was not observed as a final product. This noteworthy result reflects how the heterolytic B−X bond strength can dramatically affect the final product distribution and most importantly the formation of products that contain multiple B−H bonds. Independent syntheses and $^{11}$B NMR spectral characterization of the boron anions described in the previous paragraphs were carried out to support the proposed assignments and are described in the Supporting Information.

Reactions of B(SPh)$_3$ with three equivalents of HRh(dmpe)$_2$ yield products in which multiple B−H bonds are formed and multiple B−S bonds are broken. In these reactions, ion pairing of [H$_n$B(SPh)$_{4-n}$]$^-$ with [Rh(dmpe)$_2$]$^+$ occurs in THF, and some

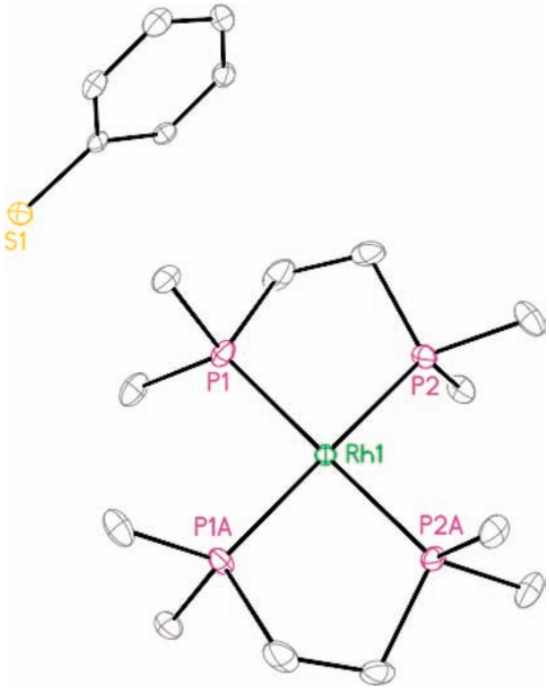

***Figure 9.*** Molecular structure of $[Rh(dmpe)_2][SPh]$ with atom numbering. Thermal ellipsoids drawn at 30% probability. Hydrogen atoms omitted.

of the displaced thiophenolate ligands form $[Rh(dmpe)_2][SPh]$. The presence of free thiolate is supported by an X-ray diffraction study of crystals grown from the reaction mixture. The molecular structure of $[Rh(dmpe)_2][SPh]$, shown in Figure 9, consists of a cationic square planar rhodium center formed by two dmpe ligands. The thiophenolate anion, located in the outer sphere, exhibits no interaction with the metal center. Metric parameters are analogous to the other cationic rhodium(I) complexes reported here. Selected metric parameters are listed in Table 3.

The facile hydride transfer from rhodium to $B(SPh)_3$ led us to explore these hydride transfer reactions in the presence of a Lewis base such as triethylamine with the intent of producing a neutral amine borane product, $Et_3N\text{-}BH_3$. Under these conditions, the presence of $NEt_3$ is anticipated to drive the reaction to the products $[Rh(dmpe)_2][SPh]$ and $Et_3N\text{-}BH_3$, as depicted in reaction 11.

$$3\ HRh(dmpe)_2 + B(SPh)_3 \xrightarrow[\text{20 equiv NEt}_3]{\text{THF, 50 °C}} Et_3N\text{-}BH_3 + 3\ [Rh(dmpe)_2](SPh) \quad (11)$$

For example, in a typical reaction triethylamine (20 equiv vs $B(SPh)_3$) was added to a THF solution of $HRh(dmpe)_2$ followed by the addition of $B(SPh)_3$. The initial $^1H$-coupled $^{11}B$ NMR spectrum recorded at 50 °C, Figure 10, trace A, indicated that $[H_2B(SPh)_2]^-$ is the principle boron species formed. In addition, several other products containing B−H bonds were identified as in the previously described reactions, including $[HB(SPh)_3]^-$, $[H_3B(SPh)]^-$, and a new product, tentatively assigned as $Et_3N\text{-}BH_2(SPh)$, which appears as a triplet at $\delta$ −6.5 ($J_{B-H} = 115$ Hz). While the initial $^{11}B$ NMR spectrum exhibits nearly identical product formation as the hydride transfer reaction in the preceding paragraph, heating of the reaction mixture at 50 °C for 14 h produced greatly different results compared to reactions without $NEt_3$. After this time, integration of the $^1H$-coupled $^{11}B$ NMR spectrum (Figure 10, trace B) indicates the product accounting for roughly 90% of the total boron in the sample is a quartet assigned to the formation $Et_3N\text{-}BH_3$. Identical $^{11}B$ NMR spectral data of independently prepared $Et_3N\text{-}BH_3$ from the addition of triethylamine to $BH_3 \cdot THF$ confirms this assignment. The remaining products identified in the $^{11}B$ NMR spectrum are $[H_3B(SPh)]^-$ ($\delta$ −25.6) and trace amounts of dmpe-$(BH_3)_2$ and $[BH_4]^-$. The presence of $NEt_3$ changes the identity of the final boron-containing products, and significantly decreases the decomposition of the $[Rh(dmpe)_2]^+$ complex by providing an alternative Lewis base to complex with $BH_3$. Furthermore, in the context of a regeneration process for AB, the formation of $Et_3N\text{-}BH_3$ provides a material suitable for a final ammoniation step, where substitution of $NEt_3$ for $NH_3$ produces $NH_3BH_3$ as the final product. Studies aimed at providing mechanistic and thermochemical information regarding the final ammoniation step are currently underway in our laboratory.

## Summary and Conclusions

Both transition metal hydrides and boron hydrides are well-known for their ability to reduce a range of organic and inorganic substrates. In this study, a previously developed scale of hydride donor abilities of a series of transition-metal hydrides in acetonitrile has been cross referenced, using $HRh(dmpe)_2$ and $[HBEt_3]^-$, to a scale of computed gas-phase hydride affinities of $BX_3$ compounds. The result is a scale that allows predictions regarding when hydride transfer should or should not occur between members of these two classes of compounds. Hopefully this scale will have applications to a broad range of problems and provide a starting point for the comparison of the hydride donor abilities of transition-metal hydrides and main group metal hydrides. We have used this scale to guide our approach to the regeneration of AB.

Approaches to the regeneration of AB from dehydrogenated material typically involve a digestion step to generate $BX_3$ compounds,[4b,5,6] which must be converted using $H_2$ back to AB. The results presented in this work demonstrate that $HRh(dmpe)_2$ can be generated from $H_2$ in the presence of a strong base, and that $HRh(dmpe)_2$ has the ability to transfer a hydride ligand to a variety of $BX_3$ compounds, including $BH_3$, $BF_3$, $HB(S_2C_6H_4)$, $B(SPh)_3$ and aryl borate esters. In the context of the regeneration of AB, choosing a $BX_3$ compound for which the resulting $[HBX_3]^-$ anions undergo ligand redistribution reactions to form species containing multiple B−H bonds is an important consideration. Our results indicate that reactions between excess $HRh(dmpe)_2$ and $BX_3$, where X = F or OAr, result in the formation of B−H containing products, but are accompanied by formation of $[BX_4]^-$, to which hydride transfer does not occur. In contrast to these findings, when X = SPh, the major products contained multiple B−H bonds, and $[B(SPh)_4]^-$ was not observed as a final product. Of particular interest to AB regeneration is the reaction of $HRh(dmpe)_2$ with $B(SPh)_3$ in the presence of triethylamine to form $Et_3N\text{-}BH_3$ in high yields, a reaction in which all B−S bonds are cleaved. Practical systems for AB regeneration will require the use of transition metal complexes using much less expensive metals than

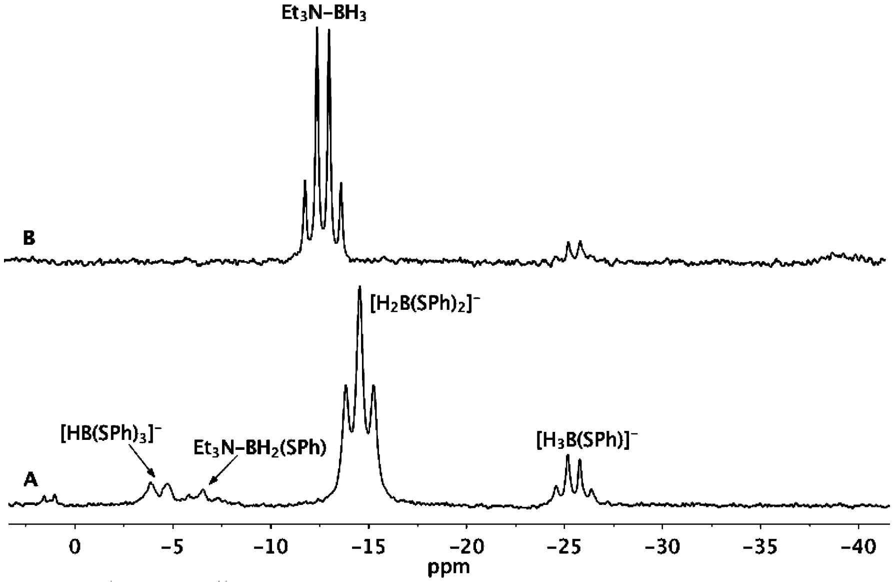

***Figure 10.*** $^1$H-coupled $^{11}$B NMR spectra of the hydride transfer reaction from $HRh(dmpe)_2$ to $B(SPh)_3$ in the presence of $NEt_3$: (A) Recorded after heating sample for 10 min at 50 °C. (B) Recorded after heating 14 h at 50 °C, showing triethylamineborane, $Et_3N$-$BH_3$ at $\delta$ −12.8.

rhodium, but the principles established here should be of use in guiding this further development.

## Experimental Section

**Computational Methods.** Electronic structure calculations using the NWChem package of programs[32] were performed to determine hydride affinities of $BX_3$ compounds in Table 1. Minimum energy structures of the boranes and their corresponding borohydrides were optimized using density functional theory,[33] the B3LYP functional,[34] and 6-311+G** basis set.[35] Enthalpies and free energies at 298 K of optimized structures were estimated from frequency calculations using the harmonic oscillator-rigid rotor approximation.

**Physical Measurements and General Procedures.** NMR spectra were recorded in thin-walled quartz NMR tubes (25 °C, unless otherwise noted) on a Varian Inova 500 MHz spectrometer equipped with a Sun workstation. $^1$H chemical shifts are referenced to residual protons in deuterated solvent. $^{31}$P chemical shifts are proton decoupled unless otherwise noted, and referenced to $H_3PO_4$ as an external reference. $^{11}$B chemical shifts are reported relative to $BF_3{-}OEt_2$ as an external reference. $^{11}$B NMR spectra were integrated to determine the ratio of total boron-containing products in solution. Infrared spectra were recorded on a Nicolet Magna 860 FT-IR spectrometer at ambient temperature and under a purge stream of nitrogen gas. Solid-state FT-IR samples were prepared as KBr pellets. Integration of $^{31}$P NMR spectral data for the $pK_a$ measurement of $[(H)_2Rh(dmpe)_2]^+$ was performed using pro-Fit software package developed by QuantumSoft.

**Synthesis and Materials.** All synthetic procedures were performed under an atmosphere of $N_2$ using standard Schlenk or glovebox techniques. Unless described otherwise, all reagents were purchased from commercial sources and were used as received. Solvents were dried by passage through activated alumina in an Innovative Technology, Inc., PureSolv solvent purification system. Deuterated THF was purchased from Cambridge Isotope Laboratories, dried over NaK, and vacuum transferred before use. Triethylamine was distilled over $CaH_2$ before use. Bis(1,5-cyclooctadiene)rhodium(I) triflate, 1,2-bis(dimethylphosphino)ethane, and Verkades base ($P(RNCH_2CH_2)_3N$ ($R = {}^i$Pr) (2,8,9-tri-*i*-propyl-2,5,8,9-tetraaza-1-phosphabicyclo[3.3.3]undecane) were purchased from Strem Chemicals, Inc. $^n$BuLi (2.5 M in hexanes), borane-dimethylsulfide, lithium hydride, and triethylamine were purchased from Alfa-Aesar. Borane−THF, 1,2-benzenedithiol, boron trifluoride diethyl etherate, and triethylamine were purchased from Sigma-Aldrich. Triethylborane (1.0 M in THF) was purchased from Acros Organics. High purity grade (99.9%) $H_2$ gas was passed through a column of Drierite before use. $[Rh(dmpe)_2][OTf]$ was prepared from bis(1,5-cyclooctadiene)rhodium(I) triflate using literature methods.[9,36] 1,3,2-Benzodithiaborolane[37] and lithium triethylborohydride[38] were prepared as described previously.

**Synthesis of $BX_3$ Compounds.** All aryl borates were synthesized from $BCl_3$ and the corresponding alcohol or thiol using a low-temperature version of the Michaelis method[39] developed by Lappert and co-workers.[40] $B(OPh)_3$ was distilled over molten sodium metal before use. $B(SPh)_3$ was prepared by adding 5 mL (48.8 mmol) of thiophenol to 16 mL (16 mmol) of 1.0 M $BCl_3$ in heptane at 0 °C. The reaction was warmed to room temperature over one hour and stirred for an additional hour. The reaction was heated at 50 °C for 12 h followed by removal of heptane under reduced pressure. The crude mixture was washed with ether (3 × 30 mL) and dried in vacuo, affording an off-white solid. Yield: 1.03 g, 19%. $^{11}$B NMR (THF): $\delta$ 62.3. $^{11}$B NMR ($CDCl_3$): $\delta$ 58.1. $^{13}$C NMR ($CDCl_3$): 134.9, 129.9, 129.0, 128.4. $^1$H NMR ($CDCl_3$): $\delta$ 7.50 (d, $^3J_{HH} = 7.2$ Hz, 6 H), 7.30 (t, $^3J_{HH} = 7.9$ Hz, 6 H), 7.23 (t, $^3J_{HH} = 7.3$ Hz, 3 H).

**Preparation of $HRh(dmpe)_2$.** $HRh(dmpe)_2$[41] was generated by adding one equivalent of $^n$BuLi (2.5 M in hexanes) to *ca.* 20−30 mg $[Rh(dmpe)_2](CF_3SO_3)$ in THF. The reaction was stirred for 30 min, and the THF was removed under reduced pressure. The remaining yellow solids were extracted with pentane or hexanes to remove $Li[CF_3SO_3]$, filtered through Celite, and dried under

---

(32) Bylaska E. J.; et al. *NWChem, A Computational Chemistry Package for Parallel Computers*, Version 5.0; Pacific Northwest National Laboratory: Richland, Washington, 2006.

(33) (a) Hohenberg, P.; Kohn, W. *Phys. Rev.* **1964**, *136*, B864. (b) Kohn, W.; Sham, L. J. *Phys. Rev.* **1965**, *140*, A1133.

(34) Becke, A. D. *J. Chem. Phys.* **1993**, *98*, 5648.

(35) Schafer, A.; Huber, C.; Ahlrichs, R. *J. Chem. Phys.* **1994**, *100*, 5829.

(36) James, B. R.; Mahajan, D. *Can. J. Chem.* **1980**, *58*, 996.

(37) Hadebe, S. W.; Robinson, R. S. *Eur. J. Org. Chem.* **2006**, 4898.

(38) Brown, H. C.; Kim, S. C.; Krishnamurthy, S. *J. Org. Chem.* **1980**, *45*, 1.

(39) Michaelis, A.; Hillringhaus, F. A. *Ann.* **1901**, *315*, 41.

(40) (a) Colclough, T.; Gerrard, W.; Lappert, M. F. *J. Chem. Soc.* **1955**, 907. (b) Colclough, T.; Gerrard, W.; Lappert, M. F. *J. Chem. Soc.* **1956**, 3006.

(41) Zargarian, D.; Chow, P.; Taylor, N. J.; Marder, T. B. *J. Chem. Soc., Chem. Commun.* **1989**, 540.

vacuum. Average yield 85%, $^1$H NMR (THF-$d_8$): $\delta$ 1.43 (m, dmpe-C$H_2$, 8 H), 1.32 (s, dmpe-C$H_3$, 24 H), −11.5 (doublet of pentets). $^{31}$P{$^1$H} NMR (THF-$d_8$): $\delta$ 26.5 (d, $^1J_{RhP}$ = 139 Hz).

**Reaction of Li[HBEt$_3$] with B(OPh)$_3$.** Li[HBEt$_3$] (2.0 mL, 1.0 mmol of a 0.50 M solution in THF) was added to 0.105 g (0.36 mmol) of solid triphenyl borate. The mixture was stirred, producing a clear solution and the reaction was monitored by $^{11}$B NMR spectroscopy. Spectral data immediately after mixing:$^{11}$B{$^1$H}, [$^1$H-coupled] NMR (THF): $\delta$ 76.5 (br, [br], Li[Et$_3$B-H-BEt$_3$]), 53.5 (br, [br], unassigned), 3.2 (br, [d], $^1J_{BH}$ = 130 Hz, [HB(OPh)$_3$]$^-$, 75%), 2.4 (s, [s], [B(OPh)$_4$]$^-$, 21%), −41.9 (s, [quintet], [BH$_4$]$^-$, 4%).

**Reaction of Li[HBEt$_3$] with B(OPh)$_3$ in the Presence of Triethylamine.** Triethylamine, 0.10 mL, was added to 2.0 mL (1.0 mmol) of a 0.50 M solution of Li[HBEt$_3$] in THF. This mixture was added to 0.121 g (0.42 mmol) solid triphenyl borate. The mixture was stirred, producing a cloudy solution. An additional 0.5 mL of THF was added to obtain a homogeneous mixture. The reaction was monitored by $^{11}$B NMR spectroscopy. Spectral data recorded after heating at 50 °C for 5 h: $^{11}$B{$^1$H}, [$^1$H-coupled] NMR (THF): $\delta$ 74.5 (br, [br], Li[Et$_3$B-H-BEt$_3$]), 53.6 (br, [br], unassigned), 11.9 (br, [br], unassigned), 3.7 (br, [d], $^1J_{BH}$ = 126 Hz, [HB(OPh)$_3$]$^-$, 72%), 2.4 (s, [s], [B(OPh)$_4$]$^-$, 26%), −12.8 (s, [q], Et$_3$N-BH$_3$, 2%).

**Reaction of HRh(dmpe)$_2$ with B(OR)$_3$, (R = Ph, C$_6$F$_5$, *p*-C$_6$H$_4$OMe).** In a typical experiment, solid B(OR)$_3$ was added to a stirring solution of HRh(dmpe)$_2$ (0.030 mmol) in 2 mL of THF. The reaction was monitored by $^{11}$B and $^{31}$P NMR spectroscopy.

Spectral data immediately after mixing with (0.014 mmol) B(OPh)$_3$: $^{11}$B{$^1$H}, [$^1$H-coupled] NMR (THF, 50 °C): $\delta$ 3.2 (br, [d], $^1J_{BH}$ = 124 Hz, [HB(OPh)$_3$]$^-$, 62%), 2.4 (s, [s], [B(OPh)$_4$]$^-$, 35%), −3.5 (d, [m], unassigned, 3%), −11.1 (s, [m], unassigned, trace amount), −38.8 (d, ($^1J_{BP}$ = 57 Hz) [m], dmpe-(BH$_3$)$_2$, trace amount). $^{31}$P{$^1$H} NMR (THF): $\delta$ 36.0 (d, $^1J_{RhP}$ = 125 Hz, [Rh(dmpe)$_2$]$^+$, 65%), 26.5 (d, $^1J_{RhP}$ = 139 Hz, HRh(dmpe)$_2$, 35%).

Spectral data immediately after mixing with (0.010 mmol) B(*p*-OC$_6$H$_4$OMe)$_3$: $^{11}$B{$^1$H}, [$^1$H-coupled] NMR (THF, 50 °C): $\delta$ 3.8 (br, [d], $^1J_{BH}$ = 105 Hz, [HB(*p*-OC$_6$H$_4$OMe)$_3$]$^-$, 40%), 2.4 (s, [s], [B(*p*-OC$_6$H$_4$OMe)$_4$]$^-$, 57%), −3.2 (d, ($^1J_{BP}$ = 57 Hz) [m], unassigned, 3%). $^{31}$P{$^1$H} NMR (THF): $\delta$ 36.2 (d, $^1J_{RhP}$ = 125 Hz, [Rh(dmpe)$_2$]$^+$, 25%), 26.5 (d, $^1J_{RhP}$ = 139 Hz, HRh(dmpe)$_2$, 75%).

Spectral data immediately after mixing with (0.010 mmol) B(OC$_6$F$_5$)$_3$: $^{11}$B{$^1$H}, [$^1$H-coupled] NMR (THF, 25 °C): $\delta$ 5.0 (br, [d], $^1J_{BH}$ = 137 Hz, [HB(OC$_6$F$_5$)$_3$]$^-$, 38%), 1.1 (s, [s], [B(OC$_6$F$_5$)$_4$]$^-$, 50%), −5.4 (s, [q], $^1J_{BH}$ = 97 Hz, [H$_3$B(OC$_6$F$_5$)]$^-$, 9%), −38.8 (d, ($^1J_{BP}$ = 57 Hz), [m], ($^1J_{BH}$ = 97 Hz), dmpe-(BH$_3$)$_2$, 3%). $^{31}$P{$^1$H} NMR (THF): $\delta$ 36.2 (d, $^1J_{RhP}$ = 125 Hz, [Rh(dmpe)$_2$]$^+$, 39%), 26.6 (d, $^1J_{RhP}$ = 139 Hz, HRh(dmpe)$_2$, 61%).

**Reaction of HRh(dmpe)$_2$ with BH$_3$·THF.** BH$_3$·THF (13 $\mu$L, 0.013 mmol of a 1.0 M solution) was added to a solution of 0.016 g (0.04 mmol) of HRh(dmpe)$_2$ in 1 mL THF. The tube was shaken to produce a clear yellow solution. The reaction was characterized by $^{11}$B and $^{31}$P NMR spectroscopy. Spectral data immediately after mixing: $^{11}$B{$^1$H}, [$^1$H-coupled] NMR (THF, 50 °C): −37.4 (s, [quintet], $^1J_{BH}$ = 82 Hz, [Rh(dmpe)$_2$][BH$_4$], 85%). $^{31}$P{$^1$H} NMR (THF): $\delta$ 37.5 (d, $^1J_{RhP}$ = 125 Hz, [Rh(dmpe)$_2$]$^+$, 35%), 26.5 (d, $^1J_{RhP}$ = 139 Hz, HRh(dmpe)$_2$ (65%).

**Reaction of HRh(dmpe)$_2$ with BF$_3$·OEt$_2$.** BF$_3$·OEt$_2$ (2.0 $\mu$L, 0.016 mmol) was added to a solution of 0.020 g (0.050 mmol) HRh(dmpe)$_2$ and 100 $\mu$L of NEt$_3$ in 1.0 mL of THF. The tube was shaken to produce a clear yellow solution. The reaction was characterized by $^{11}$B and $^{31}$P NMR spectroscopy. [Rh(dmpe)$_2$][BF$_4$] precipitates from THF during the course of the reaction affecting the integrated quantity of this product versus other observed products. Spectral data after heating 1 h at 50 °C: $^{11}$B{$^1$H}, [$^1$H-coupled] NMR (THF): $\delta$ 3.0 (d, $^1J_{BF}$ = 86 Hz, [dt], $J_{B-H}$ = 114 Hz, Et$_3$N-BH$_2$F, 37%), −1.1 (s, [s], BF$_4$, 20%), −12.8 (s, [q], $^1J_{BH}$ = 97 Hz, Et$_3$N-BH$_3$, 43%). Spectral data after heating 20 h at 50 °C: $^{11}$B{$^1$H}, [$^1$H-coupled] NMR (THF): $\delta$ −1.1 (s, [s], BF$_4$, 25%), −12.8 (s, [q], $^1J_{BH}$ = 97 Hz, Et$_3$N-BH$_3$, 75%). $^{31}$P{$^1$H} NMR (THF): $\delta$ 37.5 (d, $^1J_{RhP}$ = 125 Hz, [Rh(dmpe)$_2$]$^+$), 26.5 (d, $^1J_{RhP}$ = 139 Hz, HRh(dmpe)$_2$.

**Reaction of HRh(dmpe)$_2$ with HB(S$_2$C$_6$H$_4$).** A solution of HRh(dmpe)$_2$ 14 mg (0.034 mmol) in 2 mL THF was added to 5 mg (0.034 mmol) HB(S$_2$C$_6$H$_4$). The contents were mixed and transferred to an NMR tube affording a yellow solution with a yellow precipitate. The reaction was characterized by $^{11}$B and $^{31}$P NMR spectroscopy. Spectral data immediately after mixing: $^{11}$B{$^1$H}, [$^1$H-coupled] NMR (THF, 50 °C): 11.6 (s, [s], [B-(S$_2$C$_6$H$_4$)$_2$]$^-$, 4%), −4.7 (s, [m], unassigned, 16%), −11.5 (s, [t]$^1J_{BH}$ = 110 Hz, [H$_2$B(S$_2$C$_6$H$_4$)]$^-$, 80%). $^{31}$P{$^1$H} NMR (THF): $\delta$ 36.3 (d, $^1J_{RhP}$ = 125 Hz, [Rh(dmpe)$_2$]$^+$, 95%), 26.5 (d, $^1J_{RhP}$ = 139 Hz, HRh(dmpe)$_2$, 5%).

**Reaction of HRh(dmpe)$_2$ with Excess B(SPh)$_3$.** In an NMR tube, 10.1 mg (0.030 mmol) of solid B(SPh)$_3$ was added to 11 mg (0.027 mmol) of HRh(dmpe)$_2$ in 2 mL of THF. The tube was shaken to produce a cloudy yellow solution, and the reaction was followed by $^{11}$B and $^{31}$P NMR spectroscopy. Spectral data immediately after mixing: $^{11}$B{$^1$H}, [$^1$H-coupled] NMR (THF, 50 °C): $\delta$ 63.2 (s, [s], B(SPh)$_3$), 4.5 (s, [s], [B(SPh)$_4$]$^-$, 16%), −4.3 (s, [d], $^1J_{BH}$ = 128 Hz, [HB(SPh)$_3$]$^-$, 84%). $^{31}$P{$^1$H} NMR (THF): $\delta$ 38.2 (d, $^1J_{RhP}$ = 90 Hz, *trans*-[HRh(SPh)(dmpe)$_2$]$^+$, 2%), 35.7 (d, $^1J_{RhP}$ = 125 Hz, [Rh(dmpe)$_2$]$^+$, 98%).

**Reaction of Excess HRh(dmpe)$_2$ with B(SPh)$_3$.** In an NMR tube, 3.4 mg (0.010 mmol) of solid B(SPh)$_3$ was added to 13 mg (0.030 mmol) HRh(dmpe)$_2$ in 1.5 mL THF. The tube was shaken to produce a clear yellow solution. The reaction was monitored by $^{11}$B and $^{31}$P NMR spectroscopy while being heated at 50 °C over a period of 20 h. Spectral data immediately after mixing: $^{11}$B{$^1$H}, [$^1$H-coupled] NMR (THF, 50 °C): $\delta$ 4.5 (s, [s], [B(SPh)$_4$]$^-$), −4.3 (s, [d], $^1J_{BH}$ = 128 Hz, [HB(SPh)$_3$]$^-$), −14.5 (s, [t], $^1J_{BH}$ = 111 Hz, [H$_2$B(SPh)$_2$]$^-$). $^{31}$P{$^1$H} NMR (THF): $\delta$ 35.4 (d, $^1J_{RhP}$ = 125 Hz, [Rh(dmpe)$_2$]$^+$, 55%), 26.5 (d, $^1J_{RhP}$ = 139 Hz, HRh(dmpe)$_2$, 45%). After heating at 50 °C, 30 min: $^{11}$B{$^1$H}, [$^1$H-coupled] NMR (THF, 50 °C): $\delta$ −14.5 (s, [t], $^1J_{BH}$ = 111 Hz, [H$_2$B(SPh)$_2$]$^-$, 68%), −25.6 (s, [q], $^1J_{BH}$ = 97 Hz, [H$_3$B(SPh)]$^-$, 32%). $^{31}$P{$^1$H} NMR (THF): $\delta$ 34.9 (d, $^1J_{RhP}$ = 125 Hz, [Rh(dmpe)$_2$]$^+$, 85%), 26.5 (d, $^1J_{RhP}$ = 139 Hz, HRh(dmpe)$_2$, 15%). After heating at 50 °C, 20 h: $^{11}$B{$^1$H}, [$^1$H-coupled] NMR (THF, 50 °C): $\delta$ −14.5 (s, [t], $^1J_{BH}$ = 111 Hz, [H$_2$B(SPh)$_2$]$^-$, 11%), −25.6 (s, [q], $^1J_{BH}$ = 97 Hz, [H$_3$B(SPh)]$^-$, 68%), −38.5 (d, ($^1J_{BP}$ = 57 Hz), [m], ($^1J_{BH}$ = 95 Hz), dmpe-(BH$_3$)$_2$, 18%), −41.1 (s, [quintet], $^1J_{BH}$ = 80 Hz, Li[BH$_4$], 3%). $^{31}$P{$^1$H} NMR (THF): $\delta$ 36.4 (d, $^1J_{RhP}$ = 125 Hz, [Rh(dmpe)$_2$]$^+$).

**Reaction of Excess HRh(dmpe)$_2$ with B(SPh)$_3$ in the Presence of NEt$_3$.** Triethylamine (50 $\mu$L, 0.36 mmol) was added to 20.0 mg (0.050 mmol) of HRh(dmpe)$_2$ in 2 mL of THF and 5.8 mg (0.017 mmol) of solid B(SPh)$_3$ was added to this mixture. The tube was shaken to produce a clear yellow solution. The reaction was immediately monitored by $^{11}$B and $^{31}$P NMR spectroscopy, then again after being heated at 50 °C over a period of 14 h at which time a small amount of a yellow precipitate had formed. Spectral data recorded after heating 10 min at 50 °C: $^{11}$B{$^1$H}, [$^1$H-coupled] NMR (THF, 50 °C): $\delta$ −4.3 (s, [d], $^1J_{BH}$ = 128 Hz, [HB(SPh)$_3$]$^-$, 34%), −6.5 (s, [t], $J_{B-H}$ = 115 Hz, Et$_3$N-BH$_2$(SPh), 5%), −14.5 (s, [t], $^1J_{BH}$ = 111 Hz, [H$_2$B(SPh)$_2$]$^-$, 58%), −25.6 (s, [q], $^1J_{BH}$ = 97 Hz, [H$_3$B(SPh)]$^-$, 3%). $^{31}$P{$^1$H} NMR (THF): $\delta$ 35.1 (d, $^1J_{RhP}$ = 125 Hz, [Rh(dmpe)$_2$]$^+$, 75%), 26.5 (d, $^1J_{RhP}$ = 139 Hz, HRh(dmpe)$_2$, 25%). Spectral data after heating 14 h at 50 °C: $^{11}$B{$^1$H}, [$^1$H-coupled] NMR (THF, 50 °C): $\delta$ −12.8 (s, [q], $^1J_{BH}$ = 97 Hz, Et$_3$N-BH$_3$, 90%), −25.6 (s, [q], $^1J_{BH}$ = 97 Hz, [H$_3$B(SPh)]$^-$, 10%). $^{31}$P{$^1$H} NMR (THF): $\delta$ 34.5 (d, $^1J_{RhP}$ = 125 Hz, [Rh(dmpe)$_2$]$^+$, 95%), 26.5 (d, $^1J_{RhP}$ = 139 Hz, HRh(dmpe)$_2$, 5%).

**Determination of p$K_a$ for [(H)$_2$Rh(dmpe)$_2$][CF$_3$SO$_3$].** In a typical reaction, 1.0 mL of a 1.27 × 10$^{-2}$ M stock solution of [Rh(dmpe)$_2$][CF$_3$SO$_3$] in THF was added to a predetermined amount of VSB-$^i$pr base. The solution was mixed, transferred to an NMR tube, and sealed with a rubber septum. H$_2$ gas was purged through

***Table 4.*** Crystallographic Data for $[Rh(dmpe)_2][BH_4]$, *trans*-$[HRh(SPh)(dmpe)_2][HB(SPh)_3]\cdot THF$, and $[Rh(dmpe)_2][SPh]$[a]

| | $[Rh(dmpe)_2][BH_4]$ | *trans*-$[HRh(SPh)(dmpe)_2]$ $[HB(SPh)_3]\cdot THF$ | $[Rh(dmpe)_2][SPh]$ |
|---|---|---|---|
| empirical formula | $C_6H_{18}B_{0.50}P_2Rh_{0.50}$ | $C_{40}H_{62}BOP_4RhS_4$ | $C_{18}H_{37}P_4RhS$ |
| formula weight | 209.00 | 924.74 | 512.33 |
| color, habit | yellow, blocks | colorless, blocks | yellow, plates |
| crystal system | monoclinic | triclinic | monoclinic |
| space group | $P2/n$ | $P\bar{1}$ | $C2/c$ |
| $a$, Å | 10.4454 (1) | 13.066 (1) | 30.0678 (5) |
| $b$, Å | 9.1995 (2) | 13.086 (1) | 9.3277 (1) |
| $c$, Å | 11.4117 (2) | 13.553 (1) | 17.4534 (3) |
| α, deg | 90 | 74.795 (3) | 90 |
| $\beta$, deg | 112.762 (1) | 83.485 (3) | 100.997 (1) |
| $\gamma$, deg | 90 | 89.799 (3) | 90 |
| $V$(Å$^3$) | 1011.18 (3) | 2221.1 (3) | 4805.2 (1) |
| $\lambda$, Å (Cu (Mo), Kα) | 1.54178 | (0.71073) | 1.54178 |
| $Z$ | 4 | 2 | 8 |
| density (g/cm$^3$) | 1.373 | 1.383 | 1.416 |
| temperature (K) | 100 (2) | 100 (2) | 100 (2) |
| 2$\theta$ range, deg | 4.81−68.00 | 1.57−33.22 | 2.99−68.96 |
| $\mu$(Cu (Mo), Kα), mm$^{-1}$ | 9.685 | (0.747) | 9.062 |
| $R$(F), $R$w(F) | 0.0308, 0.0784 | 0.0260, 0.0600 | 0.0225, 0.0588 |

[a] Quantity minimized $= R(wF^2) = \Sigma[w(F_o^2 - F_c^2)^2]/ \Sigma[(wF_o^2)^2]^{1/2}$; $R = \Sigma\Delta/\Sigma(F_o)$, $\Delta = |(F_o - F_c)|$, $w = 1/[\sigma^2(F_o^2) + (aP)^2 + bP]$, $P = [2F_c^2 + \text{Max}(F_o,0)]/3$.

the reaction mixture for 2 min, and the sample was immediately inserted into an NMR probe maintained at 25.0 °C. The reaction was monitored by $^{31}$P NMR spectroscopy until the integrated ratio of $^{31}$P NMR signals for the products and reactants, $HRh(dmpe)_2$, protonated base and $[(H)_2Rh(dmpe)_2]^+$, unprotonated base, respectively, remained constant. Each reaction reached equilibrium in less than 8 h after mixing but was monitored for an additional 24 h to ensure equilibrium had been established. In order to accurately determine the equilibrium constant, due to the overlapping $^{31}$P NMR resonances of $HRh(dmpe)_2$, $[(H)_2Rh(dmpe)_2]^+$ and $Rh(dmpe)_2^+$, each of the above rhodium species was fitted to a Lorentzian function, and the best-fit data were integrated to quantify each species. The experimental procedure described above was performed using 5, 10, 20, and 40 equiv of VSB-$^i$pr, resulting in an average equilibrium constant of $(1.2 \pm 0.3) \times 10^{-3}$. The p$K_a$ of $[(H)_2Rh(dmpe)_2]^+$ was calculated by using the reported p$K_a$ of the VSB-$^i$pr in acetonitrile (33.6)[15] and the equilibrium constant measured in THF to afford a p$K_a$ value of 36.5 in acetonitrile.

**X-ray Diffraction Studies.** X-ray diffraction data were collected on a Brüker-AXS Kappa APEX II CCD diffractometer with 0.71073 Å Mo Kα radiation or 1.54178 Å Cu Kα radiation. Selected crystals were mounted using Paratone oil onto a glass fiber and cooled to the data collection temperature of 100 K. For data collection using Mo Kα radiation, unit cell parameters were obtained from 60 data frames, 0.5° Φ, from three different sections of the Ewald sphere. For data collection using Cu Kα radiation,unit cell parameters were obtained from 90 data frames, 0.5° Φ, from three different sections of the Ewald sphere. Cell parameters were retrieved using APEX II software[42] and refined using SAINT+[43] on all observed reflections. Each data set was treated with SADABS[44] absorption corrections based on redundant multiscan data. The structure was solved by direct methods and refined by least-squares method on $F^2$ using the SHELXTL program package.[45] Crystallographic data for each structure are listed in Table 4. Details regarding specific solution refinement for each compound are provided in the following paragraphs.

**$[Rh(dmpe)_2][BH_4]$.** The systematic absences in the diffraction data were consistent with the centrosymmetric monoclinic space group, $P2/n$. $[Rh(dmpe)_2]^+$ and $[BH_4]^-$ were located on special positions yielding $Z = 2$, and $Z' = 1/2$. The rhodium cation was disordered over two positions which were located from the difference map and refined using a second free variable. All non-hydrogen atoms were refined with anisotropic displacement parameters. Hydrogen atoms were treated as idealized contribution except for the hydrogen atoms from the $[BH_4]^-$ group, which were located from the difference map. $[BH_4]^-$ hydrogen atoms were allowed to refine freely except their distances were made equivalent to stabilize the refinement. The goodness of fit on $F^2$ was 1.047 with $R1(wR2)$ 0.0308 (0.0784) for $[I\theta > 2(I)]$ and with largest difference peak and hole of 0.962 and −0.520 e/Å$^3$.

***trans*-$[HRh(SPh)(dmpe)_2][HB(SPh)_3]\cdot THF$.** The data was consistent with the centrosymmetric, triclinic space group $P\bar{1}$. The *trans*-$[HRh(SPh)(dmpe)_2]^+$ cation and the $[HB(SPh)_3]^-$ anion were located on general positions yielding $Z = 2$, and $Z' = 1$. The $[HB(SPh)_3]^-$ anion was disordered over two positions (85:15) which were located from the difference map and refined using a second free variable. All non-hydrogen atoms were refined with anisotropic displacement parameters. Hydrogen atoms were treated as idealized contributions except for the hydrogen atoms bonded to Rh(1) and B(1) which were located from the difference map and allowed to refine freely. The B−H proton on the minor component of the disordered $[HB(SPh)_3]^-$ anion could not be located and was calculated using an AFIX command with the B−H distance fixed to match that of the B−H bond in the major component. The goodness of fit on $F^2$ was 1.024 with $R1(wR2)$ 0.0260(0.0600) for $[I\theta > 2(I)]$ and with largest difference peak and hole of 0.686 and −0.509 e/Å$^3$.

**$[Rh(dmpe)_2][SPh]$.** The systematic absences in the diffraction data were consistent with the centrosymmetric monoclinic space group, $C2/c$. Two $[Rh(dmpe)_2]^+$ cations were located on special positions along with one thiophenolate anion located on a general position yielding $Z = 8$, and $Z' = 1$. All non-hydrogen atoms were refined with anisotropic displacement parameters. All hydrogen atoms were treated as idealized contributions. The goodness of fit on $F^2$ was 1.029 with $R1(wR2)$ 0.0225 (0.0588) for $[I\theta>2(I)]$ and with largest difference peak and hole of 0.521 and −0.427 e/Å$^3$.

**Acknowledgment.** This work was supported by the U.S. Department of Energy's (DOE) Office of Energy Efficiency and Renewable Energy Center of Excellence for Chemical Hydrogen Storage. A portion of the research was performed using EMSL, a national scientific user facility sponsored by the Department of Energy's Office of Biological and Environmental Research and located at Pacific Northwest National Laboratory (PNNL). PNNL is operated by Battelle for DOE. The Bruker (Siemens) SMART APEX diffraction facility was established at the University of Idaho with the assistance of the NSF-EPSCoR program and the M. J. Murdock Charitable Trust, Vancouver, WA.

**Supporting Information Available:** Experimental details and NMR spectral data for the preparation of the compounds $Li[HB(OPh)_3]$, $Li[HB(SPh)_3]$, $Na[H_3B(SPh)]$, $Na[B(SPh)_4]$; full X-ray diffraction refinement data (CIF) for $[Rh(dmpe)_2][BH_4]$, *trans*-$[HRh(SPh)(dmpe)_2][HB(SPh)_3]$, $[Rh(dmpe)_2][SPh]$, $[Rh(dmpe)_2][B(OPh)_4]$, $B(SPh)_3$; NMR spectral data for hydride transfer reactions to $BH_3\cdot THF$, $BF_3\cdot OEt_2$ and $HB(S_2C_6H_4)$, results of hydride transfer from rhodium to $B(OC_6F_5)_3$ and $B(p\text{-}OC_6H_4OMe)_3$; discussion regarding formation of $[B(OAr)_4]^-$; complete ref 32. This material is available free of charge via the Internet at http://pubs.acs.org.

JA905287Q

---

(42) *APEX II*, v. 2009.3; Bruker AXS: Madison, WI, 2009.
(43) *SAINT+: Data Reduction and Correction Program*, v. 7.56A; Bruker AXS: Madison, WI, 2009.
(44) *SADABS: An Empirical Absorption Correction Program*, v. 2008/1; Bruker AXS Inc.: Madison, WI, 2008.
(45) Sheldrick, G. M. *SHELXTL: Structure Determination Software Suite*, v. 2008; Bruker AXS Inc.: Madison, WI, 2008.